

Design and Simulation of an Integrated CMG and Thruster Control System

Samuel Schreiner, Timothy Setterfield, Todd Sheerin, Morris Vanegas

Abstract—As humans continue to explore outer space, the need for long-duration Extravehicular Activity (EVA) mobility units will grow. Current jetpack technology uses only thrusters for control, which can limit EVA duration and platform stability. To augment jetpack EVA capabilities, work on incorporating control moment gyroscopes (CMGs) into a jetpack design is underway at MIT and Draper Laboratories. We present the work undertaken as a part of course 16.851 in MIT AeroAstro to lay the groundwork for a hardware demonstration of a combined CMG and cold gas thruster control system by integrating CMGs onto the Synchronized Position Hold Engage and Reorient Experimental Satellites (SPHERES) facility. The SPHERES facility currently utilizes a set of thrusters for control actuation and provides a suitable testbed for the integration of CMGs and new control algorithms. This report details the work conducted on the mechanical, electrical, and software interface design necessary to integrate CMGs onto a SPHERES satellite. Additionally, the authors describe the development of a software simulation of the SPHERES satellites with CMGs, which will allow future users to simulate and test the performance of integrated CMG and thruster control algorithms in a high-fidelity virtual environment prior to hardware testing.

CONTENTS

I	Introduction	1
I-A	Project Motivation	1
I-B	Team CMG Objectives	2
II	System Requirements	2
III	Hardware	3
III-A	Introduction and Objectives	3
III-B	CMG Background	3
III-C	SPHERES Background	4
III-D	Halo Background	6
III-E	Mechanical Design	6
III-F	Expected Performance	9
III-G	Electrical Design	10
IV	Software	13
IV-A	Software Introduction/Objectives	13
IV-B	Software Background	13
IV-C	Conceptual Software Design	14
IV-D	CMG Payload Simulation Design	14
IV-E	SPHERES Controller Software Design	15
IV-F	Simulation Results	16
IV-G	Preliminary Trade-off Analysis	17
V	Future Work	19
V-A	Air-Bearing Table Demonstration	19
V-B	Halo Hardware Development	19
V-C	Simulation Enhancements	20
VI	Conclusion	20
	Appendix A: Jetpack Development: In the Past and Today	21
	Appendix B: Alternate Mechanical Designs	21
	Appendix C: Halo Keepout Compliance	22
	Appendix D: CMG Safety Analysis	22
	Appendix E: Additional Simulation Results	25
	Appendix F: System Requirements	26
	References	27

I. INTRODUCTION

A. Project Motivation

The need for extravehicular activity (EVA) mobility units for astronauts will grow as space agencies like NASA plan human exploration missions to low gravity environments like asteroids, the Martian Moons, or man-made satellites in the Earth-Moon system. In anticipation of these future missions, NASA has placed the development of advanced human mobility units on the agency's space technology roadmap, TABS 7.3.3.4 [1]. To mature this technology, NASA has supported the development of a next-generation jetpack by an MIT-Draper Laboratory team. This jetpack design integrates control moment gyroscopes (CMGs) into a traditional cold-gas propulsion system architecture with the goal of improving jetpack stability and reducing propellant consumption [2] (*for more information about the preliminary findings of the MIT-Draper team as well as for a discussion of previous NASA jetpack programs, see Appendix A*).

As part of the MIT-Draper CMG jetpack development effort, a group in the fall 2013 MIT 16.851 class (Team CMG) has been tasked with designing and simulating a hardware demonstration of a combined CMG and cold gas jet actuation system by integrating CMGs onto the Synchronized Position Hold Engage and Reorient Experimental Satellites (SPHERES) testbed at MIT's Space System Laboratory (SSL) [3]. This development path is advantageous for the MIT-Draper team

Samuel Schreiner, Timothy Setterfield, Todd Sheerin, and Morris Vanegas are members of the CMG project group in the class 16.851 at the Massachusetts Institute of Technology.

not only because the SPHERES facility was specifically engineered to serve as a control development testbed, but also because the existing SPHERES architecture and institutional support at MIT together afford an accelerated development cycle that is by nature low-risk and low-cost. In addition, the SPHERES program has an extensive history of control algorithm development in the laboratory as well as in micro-gravity environments including both parabolic aircraft and the International Space Station (ISS) [4], providing a unique and mature infrastructure to support an experimental campaign of a CMG-integrated SPHERES system.

B. Team CMG Objectives

The primary objective of Team CMG is to enable the demonstration of integrated CMG and cold gas thruster actuation of a SPHERES satellite through system design and simulation. A secondary objective was to verify the simulated performance gains found by Carpenter et al. [5] for a CMG-integrated system compared to a thrusters-only jetpack. Of course, because a direct scaling of CMG-jetpack dynamics to the SPHERES system is not possible, only low-fidelity estimates of performance gains can be conducted.

Initially, the project's purpose was simply to enable control algorithm testing and development for a CMG-integrated jetpack. As the semester progressed, this purpose was extended to providing improved attitude control authority to future SPHERES systems augmented with multiple additional, externally mounted subsystems (the capacity of SPHERES to connect to multiple additional subsystems is currently in-development as part of the Halo project, which will be discussed later in this paper). Faced with this dual purpose, design and simulation efforts have been maximized by conducting the hardware and electrical designs on the SPHERES, Halo, and CMG system (CMG-SPHERES-Halo system) for eventual use in 3D space, while the simulation and software development focused on the initial demonstration of a SPHERES satellite (CMG-SPHERES system) operating on the SSL's air-bearing table environment.

Due to this dichotomy, hardware design presented in this report focus on the development of a CMG-SPHERES-Halo system that will ultimately be used to demonstrate combined CMG and cold gas thruster actuation in 6-DoF. This ultimate implementation will be useful both to the MIT-Draper jetpack development effort as well as to the larger programmatic goals of the SPHERES program at MIT's SSL. Software and simulation designs, on the other hand, focus on the CMG-SPHERES system to be used in initial demonstration efforts of combined CMG-thruster actuation. This initial implementation will utilize two CMGs to control 1-DoF rotation and will be tested on SSL's air-bearing table for 3-DoF (1-DoF rotation, 2-DoF translation) testing. As such, the simulation results specifically reference this testing plan.

The driving system requirements for the project are reviewed in Section II. In Section III, we cover the background of control moment gyros (CMGs), SPHERES and Halo, as well as the recommended mechanical and electrical designs. Following this, Section IV introduces the SPHERES simulation and

details the software and simulation design; preliminary simulation results and trade studies are then presented. Section V details a plan for future design, hardware implementation and experimental demonstration activities. Finally, Section VI summarizes the accomplishments of the hardware, electrical, and software design efforts.

II. SYSTEM REQUIREMENTS

Top-level system requirements for both the 2-CMG array CMG-SPHERES system and the future 4-CMG array CMG-SPHERES-Halo system are presented in this section and are compiled in table I below. For both systems considered, the SPHERES facility must retain nominal functionality including state estimation and housekeeping processes after hardware and software integration with CMGs, indicated in the table by the "SPHERES Integration" requirement. In this way, the CMG subsystem will be restricted to a modular and non-essential addition to the overall system. Modifications to the original SPHERES system should be restricted to changes committed to communication and propulsion processes that can be turned on or off to enable CMGs to share control authority with the gas thrusters on SPHERES. By adhering to this requirement, the integrity of the SPHERES system is preserved, and hardware demonstrations can directly compare system performance when functioning in a combined CMG and cold gas thruster mode as opposed to a jets-only mode of operation.

The next three general requirements listed in the Top-Level System Requirements Table I concern the performance and mission objectives of the project. CMGs have been sized for integration with the SPHERES facility so as to ensure sufficient attitude control authority to translate and rotate a 4-CMG, 6-DoF capable system for the worst-case attitude control scenario. This worst-case scenario has been identified to be the situation in which a large external mass is fixed to the system. With a mind to future experimentation in the SSL, the mass configuration corresponding to docking an inactive SPHERE satellite to the active CMG integrated satellite has been used as the worst-case scenario to size CMGs for this project. This requirement for sizing not only allows for an eventual simulation of jetpack EVA scenarios such as the rescue of an incapacitated crew member or the manipulation of heavy objects and large tools, but also will provide a large attitude control authority for a future CMG-SPHERES-Halo system augmented with large or heavy sensors. In the end, limited options for so-called "mini" CMG models forced the authors to select over-powered (Honeybee-provided) CMGs when considering CMG integrated SPHERES systems as a model for a CMG integrated jetpack.

The two mission requirements contained in the table correspond to the primary objective of designing and simulating combined CMG and cold gas jet thruster actuation of the SPHERES facility to ensure the success of a hardware demonstration. Of particular importance to note here is the requirement in the "CMG-SPHERES-Halo Mission" statement to provide variable implementation options to the user. At the very least, multiple control algorithms must be implementable.

TABLE I. TOP-LEVEL SYSTEM REQUIREMENTS. TABLE INCLUDES REQUIREMENT STATEMENTS, IMPLICATIONS ON PROJECT GOALS FOR EACH REQUIREMENT, AND THE VERIFICATION METHOD NECESSARY FOR EACH REQUIREMENT.

Requirement Type	Statement	Rationale	Verification
SPHERES Integration	SPHERES functionality must be conserved after CMG integration	State estimation must remain unchanged; comm and prop must operate as modified or in jets-only mode	Simulation, design analysis, testing
Performance (CMG Sizing)	Sufficient torque and ang. momentum for trans and rot of 2-spheres docked (4-CMG array)	Programmatic, experimental goal	Simulation and design analysis
CMG-SPHERES Mission	2-CMG array must interface directly to SPHERES or VERTIGO; 3-DoF (2 trans, 1 rot) controllable	Stepping-stone to 4-CMG array implementation; basic programmatic, experimental goal	Simulation, design analysis, testing
CMG-SPHERES-Halo Mission	4-CMG array must interface with Halo; 2x 3-DoF (2 trans, 1 rot; 3 rot), 6-DoF (3 trans, 3 rot) controllable, variable implementation	Advanced programmatic, experimental goal	Simulation, design analysis, testing

This follows from the objective of providing a control algorithm testbed for jetpack development. The design pursued by the authors also provides for two different CMG array configurations: one that is commandable with steering logic built into the Honeybee CMG controller (box 90 configuration) and one that is suited to the steering logic currently under development at Draper for the jetpack application (pyramid configuration). For reference, the experimental plan for the CMG-SPHERES-Halo system entails both flat-floor testing (3-DoF: 2-trans, 1-rot) as well as spike testing (3-DoF rotation) in the SSL before ultimately testing in a 6-DoF microgravity environment (more detailed future plans are included in V below).

It should be noted that requirements related specifically to normal SPHERES operations including state estimation, data logging and throughput requirements have not been explicitly included in this report; rather, we have chosen to identify only those system requirements that are unique to the CMG integrated SPHERES systems considered in this report.

For more detailed information about the derivation of performance requirements as well as CMG configurations, see Section III below; for more detailed information about performance and mission requirements please see the Appendix F. Also included in the appendix are requirements for CMG actuators identified by the undergraduate 16.83 class as part of their project to design a specific CMG-SPHERES-Halo system to function as an autonomous inspection unit.

III. HARDWARE

A. Introduction and Objectives

The goal of adding CMGs to SPHERES is to create a testbed for a scaled down analogue of an EVA jetpack utilizing CMGs. Valuable experience can be gained from such a hardware demonstration (utilizing thrusters and CMGs) that can contribute to implementing a CMG EVA jetpack. For this implementation, MIT's Space Systems Lab has expressed interest in mounting the CMG suite onto a SPHERES add-on

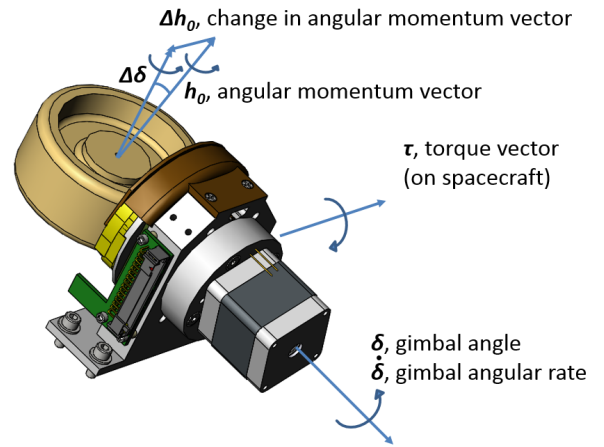


Fig. 1. The vectors involved in the operation of a CMG.

called Halo, which is currently under development. With this compatibility requirement in mind, objectives for a hardware design include using as little of the Halo real estate as possible, having CMG operation not interfere with thrusting and state estimation of SPHERES, and having an integrated system that can operate with thrusters-only and with thrusters and CMGs at the same time.

B. CMG Background

Control moment gyroscopes are used for rotational attitude control of a spacecraft. An individual CMG unit comprises a flywheel rotating at constant angular velocity; this flywheel is attached to a gimbal motor, which allows the flywheel's angular momentum vector to be rotated as desired. Rotating the angular momentum of the CMG requires that the spacecraft exert a torque on the CMG; an equal and opposite torque is thus exerted on the spacecraft. *In an inertial coordinate system*, the torque vector exerted by a single CMG on the spacecraft

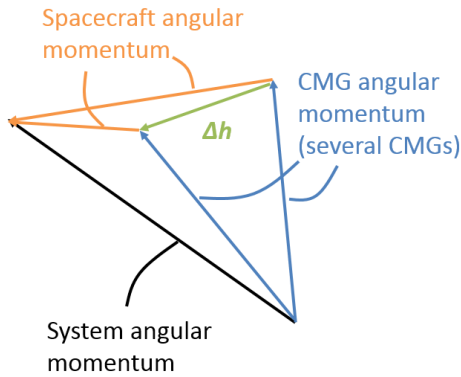


Fig. 2. The effect of CMG angular momentum on spacecraft angular momentum when system angular momentum is constant.

$\vec{\tau}_{sc}$ is then:

$$\vec{\tau}_{sc} = -\dot{\delta} \times \vec{h}_0 \quad (1)$$

where $\dot{\delta}$ is the rate of change of gimbal angle [rad/s] (herein referred to as the gimbal rate), and \vec{h}_0 is the angular momentum vector of the CMG [Nms]. The directions of these vectors for the Honeybee Robotics LEO-H120 CMG are shown in Figure 1.

Several CMGs are typically used in an array to ensure that the angular momentum vector of the CMG system can be pointed in any direction in 3D space. By combining the effects of several CMGs' angular momenta in a constructive or destructive manner, both the magnitude and the direction of the net angular momentum of the CMG array can be controlled. In the absence of external torques (due to thrusters, atmospheric drag, solar pressure, etc.), the net angular momentum of the entire system may be considered constant. This means that any change in the direction or magnitude of the angular momentum of the CMGs causes the angular momentum of the spacecraft to adjust to compensate. This concept is illustrated in Figure 2.

Several configurations of CMGs have been proposed and implemented including the scissor pair, pyramid, box 90, roof-top, and more [6], [7]. Salient features for full CMG arrays include 3 degrees of freedom (DoF) control, low mass, and redundancy in the case of CMG failure(s). At least 4 CMGs are required for 3-DoF control with a single level of redundancy. Since most of the mass of a CMG system is in the CMG flywheels, the requirement for at least 4 CMGs limits the minimum mass of a viable redundant CMG configuration. For the final hardware design to be implemented on Halo, the authors focused on two configurations: pyramid and box 90. The primary CMG array utilized in the software design was a scissor pair for its simplicity and ability to fully control rotational motion on the SSL's air-bearing table (see Section IV).

The pyramid configuration consists of 4 CMGs where the angular momentum of each CMG is constrained to one of the triangular faces of a right pyramid, as shown in Figure 3. When

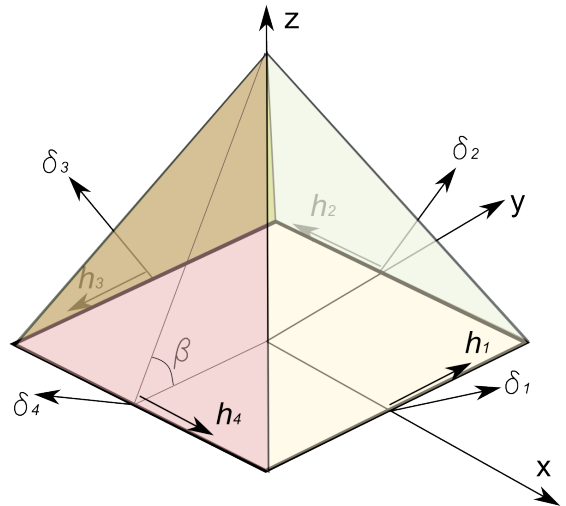


Fig. 3. The geometry of the pyramid configuration of 4 CMGs.

the pyramid angle $\beta = 54.74^\circ$ the angular momentum envelope is nearly spherical, meaning that approximately equal net angular momentum ($\sim 3.15 \vec{h}_0$) can be pointed in any direction [7], [8]. Despite this advantage, the pyramid configuration is prone to many singularities in angular momentum space, as can be seen in Figure 4. Points on the external singular surface represent the limits of the net angular momentum vector. Points on the internal singular surface represent points in momentum space that need to be avoided. The complex nature of the internal singular surface means that developing effective control laws for the pyramid configuration is still an open research problem.

The box 90 configuration is identical to the pyramid configuration, except that the angle β is increased to 90° ; this means that the faces constraining the angular momentum vectors form a box rather than a pyramid. The box 90 configuration is illustrated in Figure 5. The box 90 has an ellipsoidal angular momentum envelope ($\sim 2\vec{h}_0 \times 2\vec{h}_0 \times 4\vec{h}_0$) [7], [8]. However, it is free of the complex internal singularities present in the pyramid configuration. This means that effective control is not an open research problem; in fact, an on-board pseudo-inverse control law for the box 90 configuration is available on the Honeybee Robotics CMG control board, which allows users to directly send torque commands to the CMG control board. The external singular surface for the box 90 configuration is shown in Figure 6.

C. SPHERES Background

SPHERES (Synchronized Position Hold Engage and Reorient Experimental Satellites) is a testbed consisting of multiple self-contained satellites, each controllable in 6-DoF. SPHERES provides a long term, replenish-able, and upgradable testbed to validate high risk control, metrology, and autonomy technologies necessary for the operation of distributed satellite and docking missions. SPHERES satellites have been tested

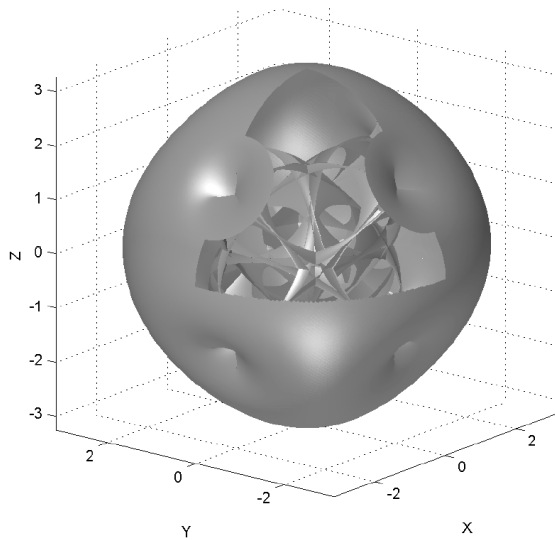


Fig. 4. The singular surfaces of a 4 CMG pyramid configuration with $\beta = 54.74^\circ$ [8]. A vector from the origin a point in this plot represents the magnitude and direction of net angular momentum for a given combination of gimbal angles $\{\delta_1, \delta_2, \delta_3, \delta_4\}$. The scale is normalized with respect to $|\vec{h}_0|$, the magnitude of angular momentum of a single CMG.

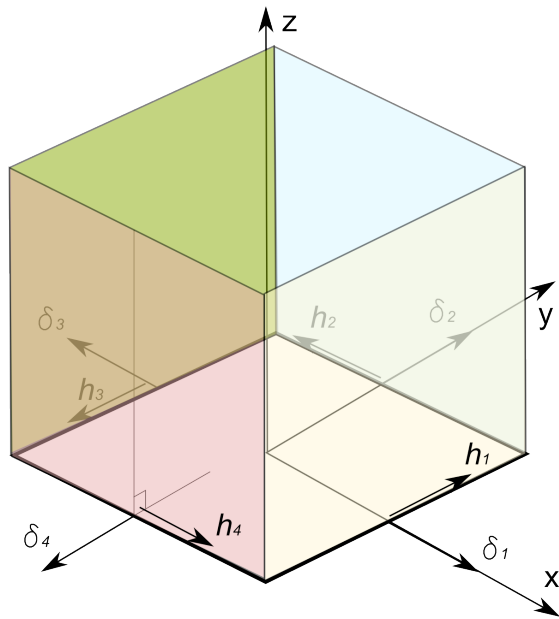


Fig. 5. The geometry of the box 90 configuration of 4 CMGs.

on the MIT Space System Laboratory's 2-D air-bearing table, on NASA microgravity flights, and on-board the International Space Station [9].

A sample SPHERES satellite can be seen in Figure 7. Each aluminum SPHERES satellite has a mass of 4.2 kg, a CO₂ tank and micro-machined nozzles for propulsion, an ultrasound ranging system with infrared triggers, a small on-board proces-

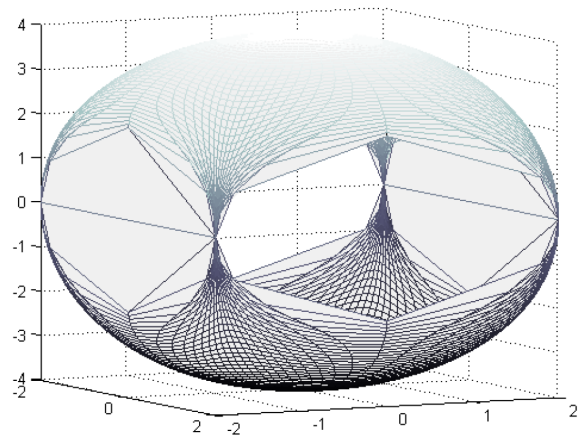


Fig. 6. The external singular surface for a box 90 configuration of 4 CMGs. The scale is normalized with respect to $|\vec{h}_0|$, the magnitude of angular momentum of a single CMG.

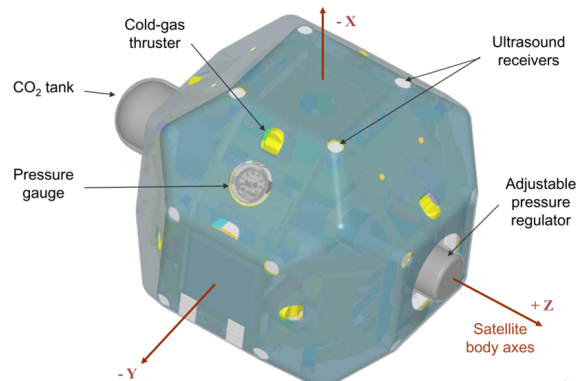


Fig. 7. A SPHERES satellite with associated body axes.

sor, an Inertial Measurement Unit (IMU) containing three rate gyros and three accelerometers, an internal replaceable battery pack, and has both SPHERE-To-SPHERE and SPHERE-To-Laptop wireless communication channels.

The SPHERES satellites use twelve cold-gas thrusters for both translation and rotational control to attain a specified attitude and position inside a test volume that is dependent upon test location (the SSL air-bearing table, a microgravity aircraft, or the ISS). Infrared (IR) pulses from SPHERES trigger static, external ultrasound (US) beacons surrounding the test volume to determine the satellite's distance from each beacon, and the SPHERES on-board computer uses this information to determine its position and orientation in space.

Each SPHERE is equipped with an expansion port used to interface with additional hardware. The expansion port allows the addition of another SPHERES satellite, payload, sensors, or actuators. In 2010, the MIT Space Systems Lab and Aurora Flight Sciences began the DARPA sponsored Visual Estimation and Relative Tracking for Inspection of Generic Objects (VERTIGO) program [10]. VERTIGO hardware is composed of a Linux computer (avionics stack) and stereo camera pair (goggles). This paper takes advantage of the



Fig. 8. The current conceptual design for Halo, shown with Halo but without peripheral payloads.

VERTIGO avionics stack's USB output to create a pass-through for information from SPHERES to the CMG control board.

D. Halo Background

As previously stated, the hardware design focused on integrating CMGs with Halo, which is currently under development in the MIT Space Systems Laboratory. Halo is an add-on for SPHERES that will increase the number of available expansion ports on SPHERES from one to six. As shown in Figure 8, the Halo structure will surround the SPHERES and provide a mechanical interface, a data connection, and power to a maximum of six peripherals. All communication with Halo peripherals will pass through the VERTIGO avionics stack, which is a powerful single-board Linux computer. An electrical port will provide USB and Ethernet data connections to the VERTIGO avionics stack, as well as power from $4 \times$ NikonE N-EL4a 11.1 V, 2500 mAh batteries. Halo will support a suite of instruments and actuators currently under development and expand the possible research activities that can be conducted on SPHERES. The hardware design presented in this paper was designed for integration with the Halo platform as part of the actuator suite.

E. Mechanical Design

The mechanical design of CMGs on SPHERES/Halo was driven by several requirements and constraints. The array of CMGs applied to SPHERES/Halo needed to be able to replicate a scaled version of typical astronaut EVA activities on a CMG+jetpack maneuvering unit. The system needed to add the minimum possible mass and power consumption, while providing redundant 3-DoF control for eventual testing

TABLE II. ANGULAR MOMENTUM AND TORQUE SPECIFICATIONS FOR THE HONEYBEE ROBOTICS LEO-H120 CMG.

Angular Momentum	
Nominal (each CMG)	0.120 Nms
Peak (each CMG)	0.160 Nms
Torque	
Nominal	0.120 Nm
Peak	0.160 Nm

in microgravity. The CMG array needed to attach to Halo and be able to perform demonstration maneuvers on the air-bearing table as well as in microgravity. As there are very few manufacturers of miniature CMGs and limited funding available for their purchase, the selection of CMGs was limited. The CMG array also needed to avoid obstructing the exhaust plume of the thrusters and the field-of-view of the US receivers so as not to disrupt the operation of the SPHERES satellite. The final conceptual design is presented in this section. Alternate designs are included in Appendix B.

Small CMGs are not a widely manufactured item. Honeybee Robotics recently developed the LEO-H120 and TORC-H86 miniature CMGs and has expressed interest in developing a working relationship with MIT and Draper Labs. Initial sizing calculations indicated that the LEO-H120 and TORC-H86 models were appropriately sized [25]. The LEO-H120 CMGs were chosen over the TORC-H86 CMGs for the Halo design due to cost reasons. The latest angular momentum and torque specifications for the LEO-H120 are shown in Table II.

The initial sizing calculations used to determine equivalence between astronaut EVA torques and SPHERES+CMGs torques is provided in the midterm report associated with this project [25]. In this analysis, the cases of an astronaut moving a 50 kg mass and an astronaut performing a quick hip-flexion motion were scaled down to the SPHERES using constant angular acceleration between the two cases. That analysis did not include Halo; nor did it include an increased torque specification for the LEO-H120 CMGs (from 0.050 Nm to 0.120 Nm). Table III shows a condensed and updated version of the scaling analysis performed in [25], including only the specifications of the selected LEO-H120 CMG. As can be seen in the table, the torque for the most extreme analogue case, hip flexion, cannot be counteracted when the inertia of Halo is included. This is acceptable since this represents a very difficult case and does not preclude interesting demonstrations with the CMGs as will be shown below.

Because of a desire to minimize the mass and power of the CMG system, only configurations with the minimum number of CMGs to enable redundant 3-DoF control were seriously considered. The two most prominent and well studied configurations in the literature that meet this requirement are the pyramid and the box 90 configuration [7], [8]. The geometry of Halo includes three sets of two parallel faces for mounting components. All faces that are not parallel are either perpendicular or at a 45° angle to each other. Given the square-base present in both the pyramid and box 90 configuration, the perpendicular faces of Halo presented the opportunity to position four CMGs in either the pyramid and the box 90

TABLE III. AN OUTLINE OF THE SCALING REQUIREMENTS FROM HUMAN AND CMG+JETPACK TO THE SPHERES WITH HALO, 4 CMGs, AND A CONTROL BOARD. PERFORMANCE OF THE LEO-H120 IN PYRAMID AND BOX 90 CONFIGURATIONS ARE CONSIDERED. * THE MAXIMUM PYRAMID CONFIGURATION TORQUE IS EQUAL TO $(4\tau_{cmg} * \sin(\beta))$. † THE MAXIMUM BOX 90 CONFIGURATION TORQUE IS DIRECTION DEPENDENT; MAXIMUMS ALONG PRINCIPAL AXES ($2\vec{h}_0$ AND $4\vec{h}_0$) AND AT 45° ($2\sqrt{2}\vec{h}_0$) ARE SHOWN.

	SPHERES/Halo, 4 CMGs, Control Board and Additional Structure
Mass	12.6 kg
Inertia (approx.)	0.237 kg m ²
Acceleration of 50 kg scenario	$\alpha \approx 0.8 \text{ rad/s}^2$, $\tau \approx 0.190 \text{ Nm}$
Hip flexion scenario	$\alpha \approx 2.6 \text{ rad/s}^2$, $\tau \approx 0.616 \text{ Nm}$
CMG torque delivered LEO-H120	0.120 Nm (max. single) 0.392 Nm (max. pyramidal*) 0.24 Nm, 0.48 Nm, or 0.34 Nm (max. box 90†)

configuration. The pyramid configuration has the advantage of a nearly spherical momentum envelope, and because its control is still an open research problem it is a fitting configuration for the SPHERES research platform. The box 90 configuration has the advantage of being free of internal singularities; also, the Honeybee Robotics CMG control board includes a built-in box 90 controller, which will make implementation easier. Due to these advantages, the decision was made to create a design that allowed for both configurations.

The final conceptual mechanical design is shown together with the SPHERES and Halo in Figure 9. The design occupies two Halo ports, with two CMGs at each port. Additionally, the top assembly includes the Honeybee Robotics LEO CMG control board. The two port design was chosen so as to keep the central port free for use as a docking port, as envisioned by the MIT 16.83 class, who will continue with the design and manufacture of the CMG system in the upcoming semester. A smaller, cubesat footprint (0.1 m × 0.1 m) control board will be released in the future by Honeybee Robotics and should be investigated prior to building the CMG system for SPHERES.

As shown in Figure 9b and c, each CMG can be attached in two orientations (by rotating the CMGs 35.26° from each other) to achieve either the box 90 (Figure 9b) or pyramid configurations (Figure 9c). The change between the two configurations is performed by unscrewing four captive screws on the mounting plates, rotating the CMG sub-assemblies, and reattaching the four captive screws (see Figure 9d and e). During this operation the CMGs are restrained by the retainers, which will prevent the CMG sub-assembly from floating away in microgravity.

The CMG system attaches to Halo's male mechanical interface with four screws. The interface is female on the CMG side, with four threaded holes on the electronics enclosure (Figure 9d) and the interface plate (Figure 9e). For the top CMG assembly, an electrical connection is made using the Halo connector (Figure 9d). This connection provides the power for the CMGs and signals for communication between SPHERES/VERTIGO and the CMG control board. A custom connector printed circuit board (PCB) is necessary to translate the USB signals from Halo to the RS-422 signals required by the CMG control board. The connector PCB will also attach to and redirect the four control board-to-CMG connections so that they exit at the connector breakouts (Figure 9d). The Honeybee LEO control board is placed upside-down to

facilitate attachment to the connector PCB and create a design that only occupies two Halo ports. The mounting plates feature an elevated platform to support the CMGs. This was included to add safety margin to the default ground clearance on the LEO-H120 CMGs.

As Honeybee Robotics does not provide enclosures for the LEO-H120 CMGs, custom covers were designed in order to contain the moving parts (Figure 9d and e). The tapered shape at the rear of the covers and mounting plates is to accommodate a slip ring that will protrude from the back of the gimbal motors. The design of this backshaft is still ongoing at Honeybee Robotics, so its length is not known. Once the information becomes available, the shape of the covers and mounting plates should be reconsidered.

The wires connecting components are not shown in Figure 9. Four connectors will exit the control board enclosure at the connector breakouts (Figure 9e); two of these will go to the CMGs located directly above and thus will only require short cables. The other two will need to pass to the other side of Halo. It may be helpful to use cable ties to organize these connections as they pass over the central Halo port. The connection to each CMG will be through a slot in the covers, visible on the bottom CMGs in Figure 9a, b, and c.

Since the CMGs will be transferring significant torques to the SPHERES, structural rigidity will be required. It is therefore recommended that all parts except for the covers and connector PCB be manufactured out of aluminum. The covers could be made out of plastic, although safety requirements for operation of flywheels on the International Space Station may necessitate a stronger material.

The masses of all major components are given in Table IV. The total mass of the designed system is 5.04 kg, not including the mass of the electronic components that will be required on the connector PCB or the mass of the wires connecting the control board to the CMGs.

The CMG system was carefully positioned so as to avoid obstructing the thrusters or ultrasonic receivers. Obstructing the thrusters would have the undesired effect of changing the direction of CO₂ flow and thus thrusting direction, which would influence control. Obstructing the ultrasonic receivers would decrease the accuracy of global metrology, which relies on ultrasonic ranging for position determination. The compliance of the CMG system with the Halo keepout zones is detailed in Appendix C.

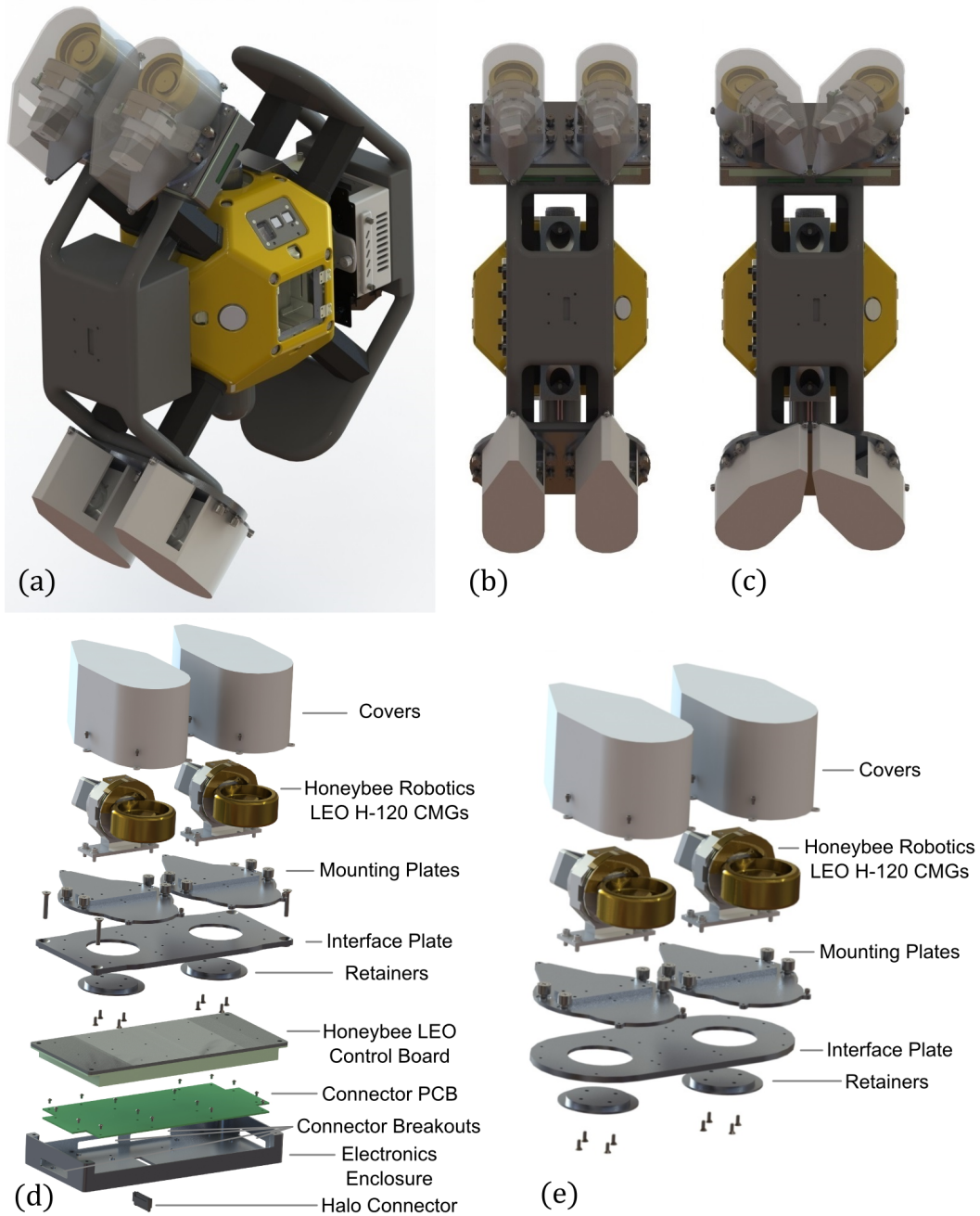


Fig. 9. The recommended CMG mechanical design for SPHERES/Halo. (a) and (b) The CMGs attached to Halo in the box 90 configuration. (c) The CMGs attached to Halo in the pyramid configuration. (d) An exploded view of the top CMG assembly. (e) An exploded view of the bottom CMG assembly.

TABLE IV. THE MASSES OF ALL MAJOR COMPONENTS EXCLUDING THE ELECTRONIC COMPONENTS ON THE CONNECTOR PCB AND THE WIRES CONNECTING THE CONTROL BOARD TO THE CMGs.

Item	Material	Mass ea. (g)	Qty.	Tot. (g)
LEO-H120 CMGs	Various	700.00	4	2800.00
LEO control board	Various	500.00	1	500.00
Mounting plates	Aluminum	122.81	4	491.24
Interface plate (control board side)	Aluminum	248.41	1	248.41
Plastic CMG covers	ABS	62.01	4	248.04
Interface plate (other side)	Aluminum	222.43	1	222.43
Electronics enclosure	Aluminum	217.88	1	217.88
Fasteners	Stainless Steel	Various	52	121.99
Retainers	Aluminum	28.52	4	114.08
Connector PCB (board only)	PTFE	74.31	1	74.31
Total				5038.38

F. Expected Performance

Given the known specifications of the LEO-H120 and the known layout of the CMGs on SPHERES, the expected performance of the CMG system can be evaluated. The volumes inside the external singular surfaces shown in Figures 4 and 6 form “angular momentum envelopes” inside which all operating points are realizable (with the aforementioned singularity restrictions in the case of the pyramid configuration). In Figure 10 a vertical plane cross-section of the angular momentum envelopes formed by the box 90 (red) and pyramid (blue) CMG arrays is shown. Points within this envelope represent directions and magnitudes of angular momentum which the CMG array is capable of achieving; points outside the envelope represent directions and magnitudes which the CMG array is not capable of achieving. The cross section for the box 90 configuration is taken so as to show its $2\vec{h}_0 \times 2\vec{h}_0$ cross-section, not its asymmetric ($2\vec{h}_0 \times 4\vec{h}_0$) cross-section (see Figure 6). The indicated operating points represent the angular velocity that the illustrated object would obtain if all of the angular momentum at that operation point was transferred to it. An angular velocity of $83^\circ/\text{s}$ is enough to saturate the rate gyroscope instruments on SPHERES, and is considered a speed limit, above which operation is not desirable. For both the box 90 and pyramid configuration, achieving $83^\circ/\text{s}$ is possible with Halo attached along the SPHERES body frame z-axis. When an air carriage (a device used to reduce the friction on the air-bearing table test facility) and its associated inertia is added to Halo, achieving $83^\circ/\text{s}$ is just out of reach of the pyramid configuration.

An interesting demonstration scenario for the CMG system is that of two attached SPHERES: one equipped with Halo, CMGs, and active thrusters; and one that is entirely passive. This scenario is meant to be analogous to an astronaut carrying an object during an EVA. For the calculations that follow, an attachment distance of 10 cm between the closest faces of the SPHERES was used. The first environment in which this scenario would be demonstrated is on the air-bearing table, so an estimated inertia of the air carriages is included in the results below. For this attached scenario, the maximum angular velocity that can be imparted about the SPHERES body frame z-axis by the box 90 and pyramid configurations is shown

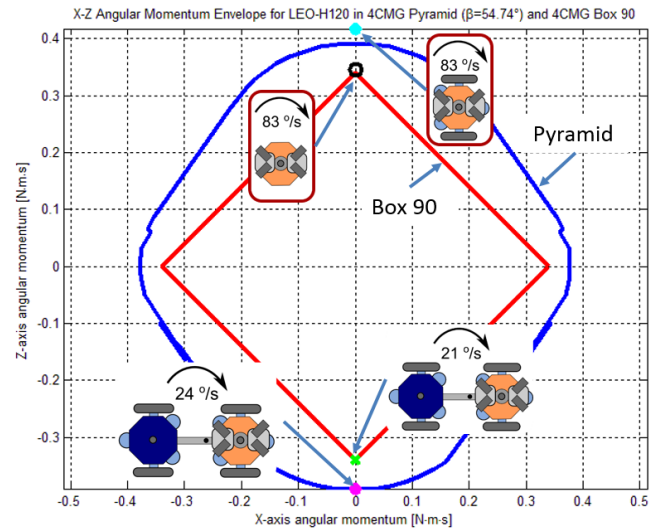


Fig. 10. The angular momentum envelopes for CMG array in box 90 ($2\vec{h}_0 \times 2\vec{h}_0$ direction) and pyramid configurations (in the SPHERES/Halo body frame x-z plane). Four points of interest are shown, representing the angular velocities achievable when all angular momentum at that operating point is imparted to the illustrated objects.

in Figure 10. For the box 90 configuration, the two attached SPHERES can achieve a maximum angular velocity of $21^\circ/\text{s}$. For the pyramid configuration, the two attached SPHERES can achieve a maximum angular velocity of $24^\circ/\text{s}$.

The attached SPHERES scenario was further analyzed to see how long the CMGs could stabilize full thrusting of the active SPHERE in a direction perpendicular to the attachment arm (Figure 11). The inertia of the passive SPHERE offsets the center of mass of the system; when the thrusters fire, this center of mass offset creates an adverse moment (an induced torque) which needs to be compensated for by the CMGs. Because of the finite magnitude of angular momentum that the CMGs can provide, there is a limit to how long this maneuver can be performed. A summary of the performance of the studied CMG arrays in this scenario is included in Table V.

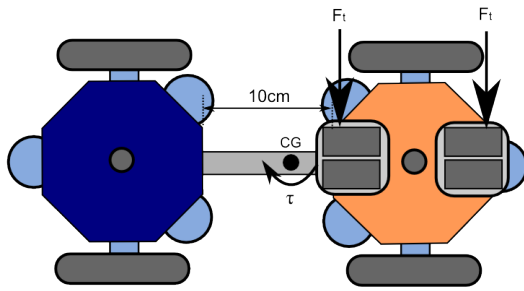


Fig. 11. A top view of two SPHERES satellites with Halo and on air carriages, attached 0.1 m apart. Two thrusters exert on the active SPHERE a force F_t , creating both an acceleration and an adverse moment τ .

TABLE V. DETAILS OF THE ANALYSIS OF THE ATTACHED SPHERES SCENARIO (FIGURE 11) INCLUDING THE PERFORMANCE OF THE CMG ARRAY. THE ABBREVIATION PYR REFERS TO THE PYRAMID CONFIGURATION AND THE ABBREVIATION B90 REFERS TO THE BOX 90 CONFIGURATION. ALL RESULTS ARE FOR THE LEO-H120 CMG.

Variable	Value
Mass of system	26.7 kg
Inertia about new center of mass (z-axis)	0.94497 kg m ²
Center of mass (x-axis, primary sphere)	+0.15634 m
Duty cycle	40%
Thruster force F_t	0.098 N
Net force ($2 \times F_t \times 0.4$)	0.0784 N
Duration of compensation	47.0 s (pyr) 40.7 s (b90)
Distance of travel	3.24 m (pyr) 2.43 m (b90)
End velocity	0.138 m/s (pyr) 0.120 m/s (b90)

G. Electrical Design

The schematic in Figure 12 shows the electrical path from SPHERES to the CMGs. Since the output of Halo is USB and the expected input of the CMG controller is RS-422 protocol, an adapter has to be incorporated to ensure the communication protocols of the two serial interfaces are compatible. The interface protocol will change from RS-232 between SPHERES and VERTIGO to USB as a Halo output to RS-422 as a controller input. The schematic also shows that the CMGs will be powered by the four external Li-ion Nikon batteries located on Halo (Nikon model EN-EL4a) that provides 11.1V and 2500 mAh of power each. The following sections will describe the electrical interfaces between systems that make communication between SPHERES and the CMGs possible. This section, however, will be limited to describing only the pins on the system pin layouts that will be used for this project. For a full description of the 50-pin connections, see the Interface Control Document for a specific system [11] [12].

1) *SPHERES Expansion*: The SPHERES expansion port is composed of an expansion PCB with a mating connector and a mounting plate. For protection, the assembly also includes a

PCB board carrier and an expansion cover used to cover the electronics when the satellite is not in use. The SPHERES expansion port mounting plate can be seen in Figure 13 along with a 50-pin connector. The expansion port mounting plate is an aluminum plate with four captive thumbscrews. The thumbscrews are used to quickly attach payloads to a SPHERES satellite.

The SPHERES Expansion Port has the capability to transmit multiple General Purpose Input/Output lines (GPIO), SPHERES reset signals, IR (infrared) and US (ultrasonic) bypasses for both sensors on SPHERES and those sensors on the payload, RS-232 and RS-422 Universal Asynchronous Receive/Transmit (UART) signals, and power (Figure 14). There are also five pins that are not currently used to allow for the interfacing with future technology. For this particular project, the following pins in the SPHERES Expansion Port will be utilized:

- +5VDC and Ground (pins 42, 44, and 30, 40, or 50)
- Basic UART RS-232 serial port (pins 14 and 16)

The 16 AA batteries inside SPHERES are capable of providing ± 15 VDC, +5VDC, regulated +3.3VDC, and ground connections. The maximum amp limit is 0.5 amps, leading the team to use the Li-ion batteries on Halo to power the CMGs rather than the SPHERES batteries. Using +5VDC and ground for handshaking from SPHERES ensures and simplifies compatibility with USB further down the electrical interfaces.

This project takes advantage of the RS-232 serial communication capability on SPHERES. Rather than sending streams of bytes, UART converts bytes into a serial stream of bits (Ones and Zeros) with organization that includes a stop and start bit in each packet of data sent.

2) *VERTIGO Expansion*: The VERTIGO avionics stack is attached to the SPHERES expansion port via 4 threaded holes on the VERTIGO internal side that match the expansion port thumbscrew pattern on SPHERES. The VERTIGO expansion port side also has 4 threaded holes (albeit, a different pattern than on the internal side) to attach payload. VERTIGO covers IR and US sensors, so the sensors had to be replicated via pass-throughs. Figure 15 provides an illustration of the configuration on the external side of the VERTIGO stack.

The VERTIGO expansion port has the capability to transmit in Ethernet and USB protocol, can receive in RS-232 and RS-422, can transmit bypass signals for sensors on its payload, forwards SPHERES commands, and can transmit power from an external battery. For this project, the following items in the VERTIGO expansion port will be utilized:

- +5VDC and ground (any of the associated pins)
- Message input from SPHERES (pin 28)
- IR and US bypass sensor pins (pins 23, 25, 27, 29, 31, 33, 35)
- USB TX and RX (pins 16 and 18)

The VERTIGO avionics stack is powered through an external Nikon battery, as described at the beginning of this section. USB communication will take advantage of the +5VDC and ground from this single battery, as well as one of the four possible USB pair connections coming from the VERTIGO expansion port (Figure 16).

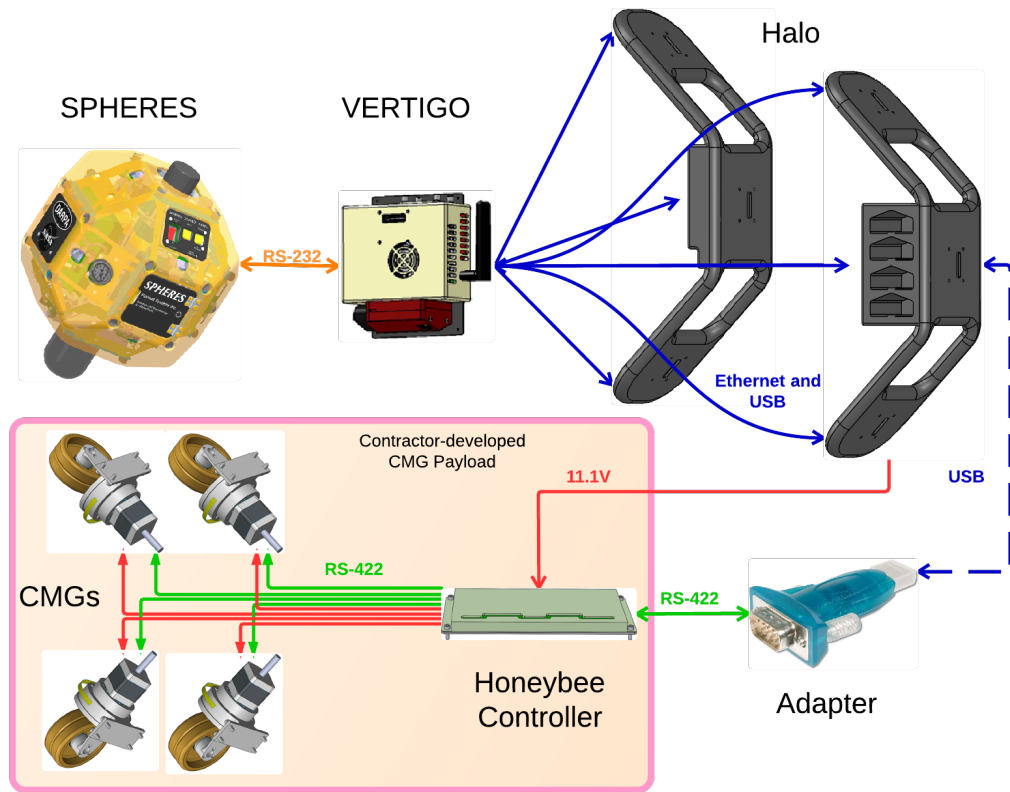


Fig. 12. Electrical Interface Schematic showing path of information and power from SPHERES to CMGs

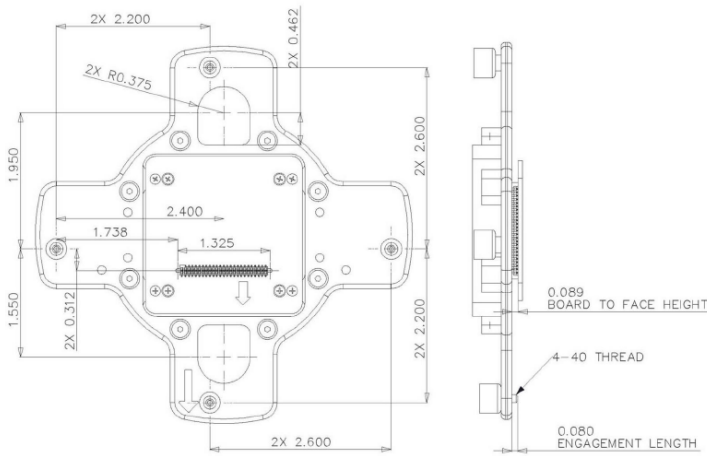


Fig. 13. A detailed view of the expansion port aluminum plate dimensions and the 50-pin connector.



Fig. 14. SPHERES expansion port electrical interface pin assignments.

Commands from SPHERES into VERTIGO will utilize the RS-232 protocol, which VERTIGO is configured to accept. As is the case with SPHERES, VERTIGO will use the IR and US bypass sensors lines because the hardware covers the "Keep out zones" on the expansion side of SPHERES (Figure 26.

3) Halo Expansion: The Halo system attaches directly to the four threaded holes on the external side of the VERTIGO avionics stack. In order to provide maximum compatibility with current payloads, each of the 6 expansion ports of Halo will also have the same physical external configuration as

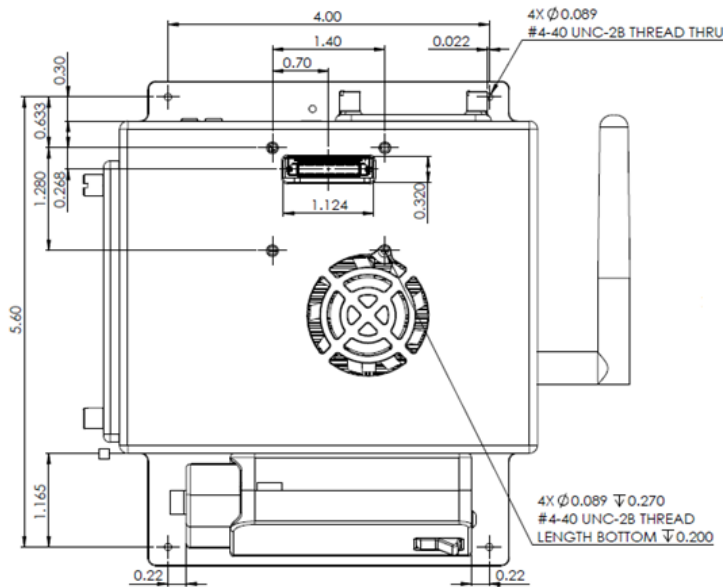


Fig. 15. Expansion side of the VERTIGO avionics stack showing four threaded holes for captive thumbscrews and a 50-pin connector.

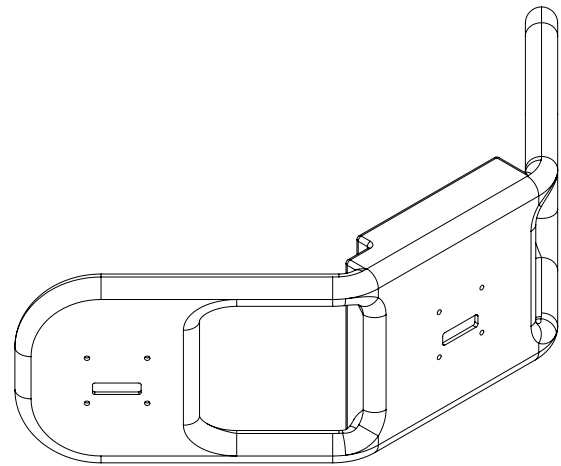


Fig. 17. Halo expansion side showing four threaded holes for captive thumbscrews and a 50-pin connector.

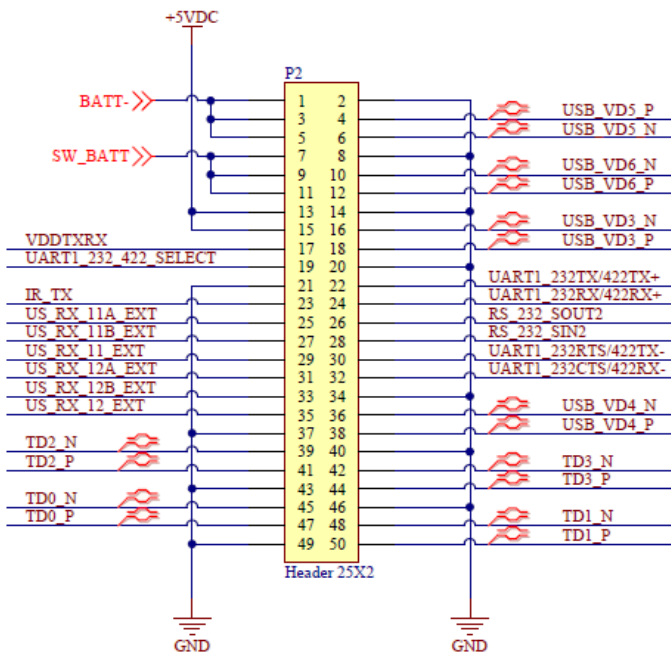


Fig. 16. VERTIGO expansion port electrical interface pin assignments.

VERTIGO (Figure 17). Thus, Halo has four threaded holes in the same pattern as the VERTIGO expansion side to interface with payloads that have previously been attached to VERTIGO. In addition, each expansion port of Halo also has four captive thumbscrews on each face, making it modular for both male and female payload connections.

Halo increases the number of expansion ports of VERTIGO from 1 to 6. In doing so, the information from SPHERES sent

to VERTIGO must be relayed to all faces of Halo. Since the commands are only being relayed, the pin layout for Halo is very similar to the pin layout for VERTIGO shown in Figure 16. The exception is that, rather than accepting RS-232 serial commands, the same pins on Halo accept USB commands because VERTIGO does not provide RS-232 output.

In addition, Halo houses four batteries on one of its two halves (The left side of Figure 8). While the single battery on VERTIGO is used to power the VERTIGO computer, the four batteries housed in the Halo structure are used to power the CMGs. We decided to use USB rather than Ethernet in Halo. Although an Ethernet communication provides faster speeds than USB, implementation is more difficult. An Ethernet-to-serial connection requires large hardware that needs its own external power. The extra bandwidth is not worth the complexity of creating an adapter between two different communication protocols. A USB-to-RS-422 connection is simpler and requires smaller hardware. This USB communication is slower than Ethernet, but faster than RS-422, which is the limiting speed in the SPHERES-to-CMG communication path. It should be stated that USB is known to have unknown latency issues. While we do not expect this latency to affect our communication significantly, testing should be conducted to determine exactly how much latency is present with this adapter. Despite this, since the CMGs require a serial RS-422 protocol, the decision to use USB protocol as the output from Halo was made due to the similarity in protocols along with the simplicity and small hardware necessary for implementation.

4) *USB Adapter:* Since the output of Halo will be USB, an adapter needs to be included in order to convert the information into an RS-422 protocol for the CMG controller board. For the ground test, this will be accomplished with a commercial-off-the-shelf USB-to-DB9 adapter. The chip receiver associates the four USB inputs into output pins with the ability to respond to CTS (clear to send) and RTS (request to send) flow control signals necessary for both RS-232 and RS-422 handshaking communication. These 9 pin outputs will then be

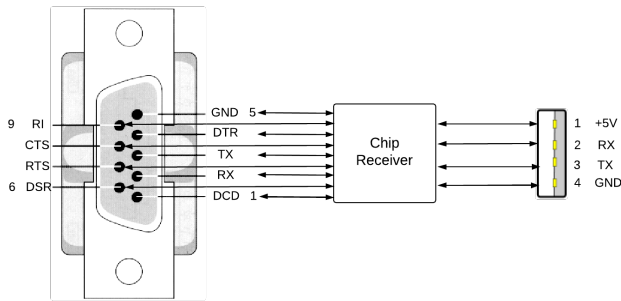


Fig. 18. USB to db9 serial adapter pin assignments.

hardwired to the CMG controller board (Figure 18). The CMG controller board can accept either torque triples for a box-90 configuration or gimbal rates for any other configuration. In the final implementation of this design, a PCB board will replace the bulky adapter. Future work needs to be completed to design this PCB and ideally place it inside the CMG controller to minimize the real estate used on the Halo faces.

IV. SOFTWARE

A. Software Introduction/Objectives

A key component of any control system is the software used to manage the system. The software developed to manage the entire SPHERES-CMG system was not written “from scratch”, as such an undertaking was beyond the scope of this course. Rather, the existing SPHERES controller code was extended to operate the CMGs as an additional actuator in the control loop. That is to say, additional code was written to execute on the SPHERES processor that is responsible for interfacing with the secondary controller embedded in the CMG payload. The holistic system utilized the existing thrusters on SPHERES for translational control and the Control Moment Gyros for attitude control.

There were several high-level software objectives. The primary objective of the software team was to create a simulation of the SPHERES + CMG system by integrating a CMG model with the existing SPHERES simulation. The simulation had to be flexible to enable the testing of multiple control schemes and allow users to implement unaltered operational flight code. The new CMG software had to operate quickly enough to not impede the existing thruster control loop. Second, the CMG software had to work effectively within the existing priority-based multithreaded environment. That is, given the fact that multiple processes are attempting to run throughout the control cycle, the CMG control code had to operate often enough to maintain control authority. Finally, the CMG control code on SPHERES had to interface with the contractor-built controller which manages the inner control loops of the CMG payload to ensure safe and reliable operation of the CMG payload.

As stated in Section I, although the end programmatic goal is to construct a system that uses CMGs to control all three rotational degrees of freedom, the initial software design focused on operating on the SPHERES air-bearing table

test facility. This initial software development will serve as a stepping stone to test the integration of the CMG payload and the SPHERES testbed. The software development focused on the air-bearing table demonstration due to the simplicity of only controlling one rotational degree of freedom (DoF) around the upward-pointing z-axis, rather than all three. Testing the software in this simpler configuration allowed for straightforward debugging and provided an avenue to directly test the software that will be used on the air-bearing table tests.

B. Software Background

To design the software in parallel with the hardware, it was decided to develop and test the software in a virtual simulation. The high-level goal of the simulation was that it provide a testbed for future users to test control algorithms utilizing both CMG and thruster actuators. The simulation was built from an existing simulation of the SPHERES satellites (using thrusters only) previously developed by the SPHERES team. This simulation takes the code written to run on the SPHERES processor (written in C) and integrates it into the Simulink simulation. This allows users to test flight software in its unaltered form in a high-fidelity environment.

A simplified version of the SPHERES controller (which is replicated in the simulation) is depicted in Figure 19. Beginning in the top left and going clockwise, the satellite’s internal estimate of its state (linear and angular position and velocity) is compared to the target state. The difference is fed to the control law which calculates the force and torque vectors required to bring the satellite to the target state. There are a wide variety of control laws, but we limited the design to a Proportional-Differential (PD) linear control law and a Non-Linear PD (NLPD) attitude control law [13]. The force and torque vectors from the control law are fed to the mixer, which determines how to fire the thruster array to achieve the desired forces and torques. The thrusters then actuate, producing a net force and torque (not necessarily equal to those commanded by the control law due to thruster noise) which act upon the satellite body. The dynamics block represents the change in state of the satellite body, which is measured by the Inertial Measurement Unit (IMU) containing accelerometers and gyroscopes. SPHERES also has sensors that receive beacon pulses from externally-mounted transmitters (“beacons”) and function in a manner similar to GPS [3]. Finally, the state estimator utilizes the sensor inputs (using an extended-Kalman filter [13]) to create a new estimate of the satellite’s state. The loop then repeats.

In Figure 19, the grey blocks are implemented in the control code (written in C) on-board the SPHERES satellite and as such, when the controller code is integrated into the Simulink model these functions are included into the simulation. The green blocks represent hardware components that had to be simulated in the Simulink model outside the controller code.

The SPHERES simulation generates an animation of the satellite maneuvers to aid users in qualitatively evaluating the performance of their controller. Furthermore, the simulation logs a multitude of variables throughout the simulation, including the satellite state vector, propellant usage, and thruster

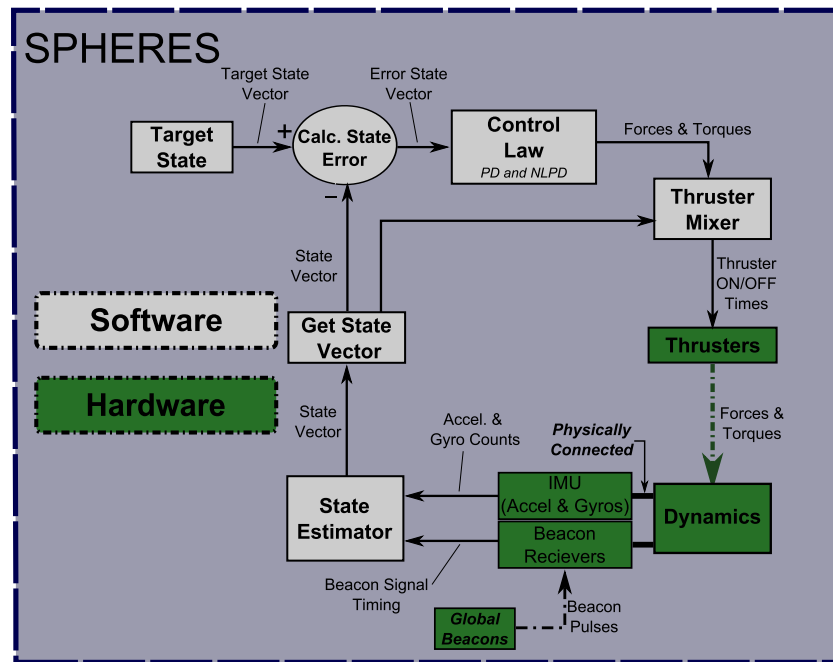


Fig. 19. A simplified depiction of the control loop on the SPHERES satellite including the key elements or “blocks”. Additionally, the type of data exchanged between each block is shown. The blocks in grey are implemented in the controller software, while the green blocks are hardware components that had to be simulated.

firing times. These variables allow users to quantitatively assess their control algorithm.

C. Conceptual Software Design

Now that we have introduced the software objectives and the existing SPHERES simulation, we will discuss the conceptual (high-level) software design used to integrate a CMG array into the SPHERES control code and simulation. Figure 20 illustrates the conceptual design used to extend the SPHERES controller code to command the CMG payload. The nominal controller logic was designed such that the CMGs are solely responsible for actuating attitude control and the thrusters are solely responsible for translation control. In the controller design, this amounts to the “Mixer” block routing force commands to the thruster array and torque commands to the newly created “CMG Payload” actuator. This scheme was chosen due to its simplicity in implementation, as well as its utility as a stepping stone for expanding CMG-thruster cooperation. That is, it is easier to troubleshoot end-to-end system bugs with a simple control scheme and it is relatively straightforward to implement more complex control schemes once the simulation is operational.

Here we describe the changes from the original control loop (shown in Figure 19) in more detail. Starting at the “Control Law” block, the torque vector is now directed to the CMG actuators while the force vector is still directed to the thrusters. Moving further around the control loop, we see the control torque vector fed to a CMG Mixer, which either commands a gimbal rate for each CMG or a three-element torque vector depending on the control method chosen. The

CMG payload receives the gimbal rate or torque commands and enacts a torque on the dynamics block. It should be noted that the thrusters still enact a torque on the dynamics block, due to residual torques from off-axis net forces. The elements discussed in Figure 19 then serve to close the control loop and provide control authority using the thrusters and CMG payload.

D. CMG Payload Simulation Design

It was necessary to design a simulator for the CMG payload in the simulation that acted according to information supplied by the contractor. For the initial simulation, a simple scissor pair CMG array was simulated. This particular CMG array was chosen due to its simplicity, but also because it provides rotational control about one axis. This provides full functionality on MIT Space System Lab’s air-bearing table, which allows the SPHERES satellites to move about two translational DoF and one rotational DoF [3].

The simulation was designed to replicate realistic communication interactions between the payload and the SPHERES controller. For instance, the simulation does not simply send a set of three numbers to the payload as a torque triplet command. Instead, the SPHERES controller converts the three values of the torque triplet to serial byte data and appends the appropriate communication protocols at the beginning and end of the message before sending the data across a simulated data bus. This includes adding the correct start byte, message ID, and message length identifier to the beginning of the message. The SPHERES simulation also has existing subroutines that allow the user to set the number of stop bits and parity bits,

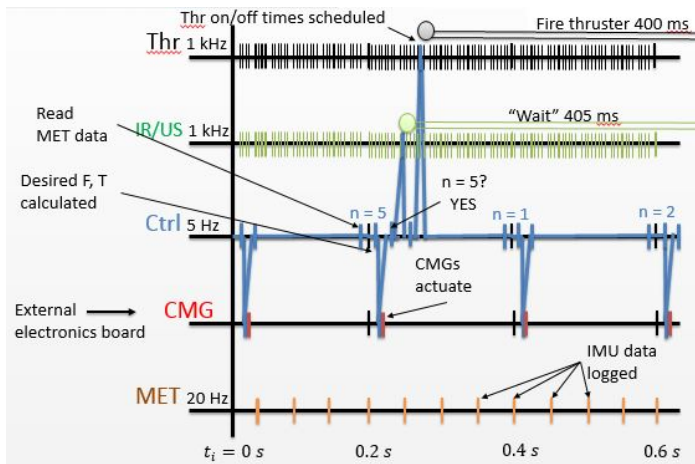


Fig. 21. The action of a 5 Hz control thread (represented by a solid blue line) is traced. It first accesses data from the metrology thread, then commands the CMG thread (running on the CMG control board); every fifth cycle, it commands thrusters after first commanding the infrared/ultrasound thread to cease global metrology in preparation for thruster actuation.

or loss of real-time control. With this in mind, we present an expanded view of the control loop as it accesses data from, and commands, other threads. The control scheme currently programmed in the simulation is depicted in Figure 21. In this figure, the control thread operates on a 5 Hz cycle, actively engaging with the metrology thread that logs IMU data at 20 Hz and Beacon data at approximately 5 Hz. To maintain the standard 1 Hz thruster control cycle on SPHERES, the thrusters are only commanded every fifth cycle ($5 \text{ Hz} \div 5 = 1 \text{ Hz}$). The reason we command CMGs at a faster rate than thrusters is to ensure that high-frequency CMG operation can compensate for unwanted torques arising from thruster actuation. Also, by maintaining thruster actuation at 1 Hz, adequate time can be provided for global metrology, which cannot function while the thrusters are firing due to the ultrasonic interference from the thruster noise [3].

The control thread schedule as presented in Figure 21 is but one implementation method possible. In one of the cycles depicted, the controller first reads IMU data from the metrology thread and performs control logic to determine torque and force measurements to achieve a certain state vector commanded by the user. Following this, the controller commands CMGs to actuate and then checks to see if thrusters should be actuated or not to maintain a 5-to-1 ratio of CMG-to-thruster actuation (if the control cycle were instead chosen to be 3 Hz, this ratio would change accordingly). If thrusters are not to be fired in the cycle, nothing more is done; but if thrusters are to be fired, the command thread first commands the infrared/ultrasound thread to wait for a period of time to ensure that thruster actuation doesn't interfere with global metrology. Following this, the controller provides thruster on and off times for the thruster thread, and then returns to await the beginning of the next cycle.

Before such a control schedule can be implemented, further analysis must be completed, foremost of which is a stability

analysis to determine an optimal control cycle rate given an IMU data logging rate of 20 Hz. In addition, a stability analysis must be performed to determine the best CMG-to-thruster actuation ratio, given metrology constraints and attitude stiffness requirements for the CMG-SPHERES platform.

F. Simulation Results

After successfully modifying the existing SPHERES simulation to include CMGs, two different sets of maneuvers were simulated and analyzed. These simulations were used to compare the performance of the SPHERES-CMG system to that of the SPHERES system alone. It should be noted that the purpose of presenting these simulations is not to say they are perfect representations of their real-world analogues, but rather that they demonstrate how the simulation can be used to analyze the possible performance improvements from adding CMGs to a cold gas thruster system. The first simulation represents the performance of the CMG-SPHERES system conducting a simple translation when a large external mass – in the form of a docked SPHERE satellite – is fixed to the system; the second simulation represents the performance of the CMG-SPHERES system alone conducting multiple maneuvers.

1) *Docked SPHERES Maneuver*: The first considered scenario simulates the situation in which an active CMG-SPHERES system is docked to an inactive SPHERE satellite on the MIT SSL air-bearing table. The mass configuration tested in this simulation corresponds to the “worst-case” attitude control scenario that initially motivated CMG sizing activities (for more information, see Sections II and III above). This docked system is commanded to translate in a direction perpendicular to the docking axis a distance of 0.5m from the starting position. Because the center of mass of the system lies outside the active SPHERE satellite, linear translation without rotation requires an attitude control effort to counter induced torque on the system.

In order to compare the performance of combined CMG and jet actuation as opposed to jets-only actuation, the same maneuver is completed for both modes of operation. Quantitative values of interest are calculated and plotted by a Matlab routine to aid analysis. In particular, linear and angular position as well as linear and angular velocity as functions of time are plotted in addition to propellant usage and CMG gimbal angles for both modes of operation in the same test scenario. To supplement plotting results for trade analysis purposes, the same routine provides a preliminary indication of performance gains characterized by increased EVA times and mass savings that are enabled with CMG operation of a scaled system (for more about preliminary trade analysis results, please see below).

Not surprisingly, if the nominal position and attitude control algorithms are implemented with this new configuration, the jets-only mode of operation fails to perform the maneuver as commanded and instead allows for the CMG-SPHERES system to enter into a spin resulting from the induced torque caused by the new center of mass of the system; the CMG+jets mode of operation, by comparison, successfully performs the maneuver. By increasing the positional and especially the

attitude controller algorithm gains for the jets-only mode of operation, performance can be improved at the expense of fuel consumption, enabling a successful maneuver. Importantly, though, there is a limit to the increase in performance possible tracing back to the limited duty cycle of the gas thrusters of SPHERES. This limit is evidenced by the nearly identical performance of the system when position and attitude gains are multiplied by 6 and 250, respectively as compared with 3 and 75 (nominal gain is the case where position and attitude gains are multiplied by unity). This implies that maximum performance is attained by using gains that are multiplied by 3 and 75 in the jets-only mode of operation for this maneuver (for analytical plots depicting this maximum performance measure, please see the appendix, Section E).

Instead of comparing the maximum performance of jets-only operation with the best performance of a CMG+jets mode of operation, the authors have elected to tailor the position and attitude control algorithm gains of the CMG+jet mode of operation so that performance approximates that of the jets-only case. In this way, a clear indication of the effect of CMG operation in the CMG-SPHERES system can be discerned. As expected, while the CMG+jets mode of operation performs nearly identically to the jets-only mode of operation (as designed for the simulation), fuel consumption is reduced dramatically – in this case, by 76%. For Matlab plots corresponding to this comparison, please see Appendix E. For analytical plots depicting this simulation’s results, as well as for a simulation that uses proper position and attitude gains to achieve the best CMG+jets performance instead of just equivalent performance to the jets-only operation, please refer to the appendix, Section E.

2) *Astronaut EVA Maneuver*: The second set of maneuvers was intended to represent an astronaut conducting an extravehicular activity (EVA) servicing mission to two different locations on the International Space Station. Figure 22 depicts the maneuver, in which the SPHERES satellite (our “astronaut”) moves out to one node and conducts some maintenance activity that requires rotation. Next, the astronaut moves to a second node and conducts more activity that requires rotation. Finally, the astronaut returns to the airlock and turns to correctly orient him/herself to reenter.

As described above, a Matlab routine was written to plot some of the quantitative data from the simulation, such as the linear and angular position, as well as the linear and angular velocity. To aid in the trade-off analysis, we also plotted propellant usage and the CMG gimbal angle. These two metrics gave us insight into how much the controller was using the thrusters and CMGs. All of these variables were plotted for a SPHERES+CMG simulation as well as a simulation of the SPHERES using thrusters only in Figure 23.

In Figure 23, the combined CMG-thruster system (“*CMG-JET*”) displays more precise performance in its angular position and velocity. This is not necessarily a significant result. Rather, this results from the CMG payload being able to exert higher torques than the thrusters. Furthermore, there was no noise or latency built into the simulated CMG payload. For example, it instantly was able to generate the torque when it received a command. The more important result is in the

propellant used graph in the bottom left, which clearly demonstrated the propellant savings achieved when using CMGs for attitude control. In the case of this particular maneuver, we observed a 39% reduction in fuel usage.

G. Preliminary Trade-off Analysis

In the final design of an EVA maneuvering unit, it will be necessary to conduct a comprehensive trade study of the mass, volume, power, performance and complexity of the unit with and without CMGs. The question remains as to whether increased platform stability, a reduced risk of thruster gas impingement on sensitive work stations, and decreased propellant consumption outweigh the increased complexity and mass requirements incurred with the addition of the CMG system. Although this trade study is beyond the scope of our project, we conduct here a high-level, first-order trade study of the SPHERES facility with and without CMGs, presented in Table VI.

Mission Duration Increase: The clearest, most transferable result from our study is that a CMG integrated system uses less propellant than the thrusters-only system. This implies that a CMG integrated EVA maneuvering unit could be used for longer duration EVAs and might also benefit from mass savings derived from propellant and tank mass reduction. Of course, any calculation of mass savings must take into account the additional mass of the CMG payload and required batteries and electronics to operate the CMG payload. Because the CMGs used for this project are much larger than the SPHERES facility requires, a direct mass trade-off is not appropriate. Instead, we attempt to scale down the mass of the CMG payload to approximate the mass of an appropriately-sized CMG payload that could achieve the same performance.

For this trade-off analysis, the mission duration capability $T_{mission}$ is calculated by determining how long the given maneuver could be repeatedly carried out before exhausting the SPHERES propellant tank:

$$T_{mission} = \frac{Tank\ Capacity\ (172g)}{Propellant\ for\ 1\ maneuver} \times T_{Maneuver} \quad (2)$$

where $T_{Maneuver}$ is the time to complete 1 maneuver. Comparing these calculations for the thrusters-only and combined CMG-thruster systems, we observed a 325% increase in mission duration from 0.7 hours to 3.0 hours for the ‘Docked’ SPHERES maneuver and a 64% increase from 2.3 to 3.8 hours for the astronaut ‘EVA’ maneuver (see Table VI). For both cases, batteries with large enough energy capacity are assumed to be used such that propellant limits mission time as opposed to CMG battery life.

Preliminary Mass Trade Analysis: In addition to the mission duration analysis, a preliminary mass trade-analysis was conducted. The first step was to calculate the mass of propellant saved by using CMGs rather than thrusters for rotational commands. Figure 24 shows the amount of propellant used in the analogue ‘EVA’ maneuver simulation for the thrusters only (red solid line) and for the integrated thruster and CMG controller (blue dashed line). To calculate propellant used, the cumulative thruster-open time was multiplied by the mass flow

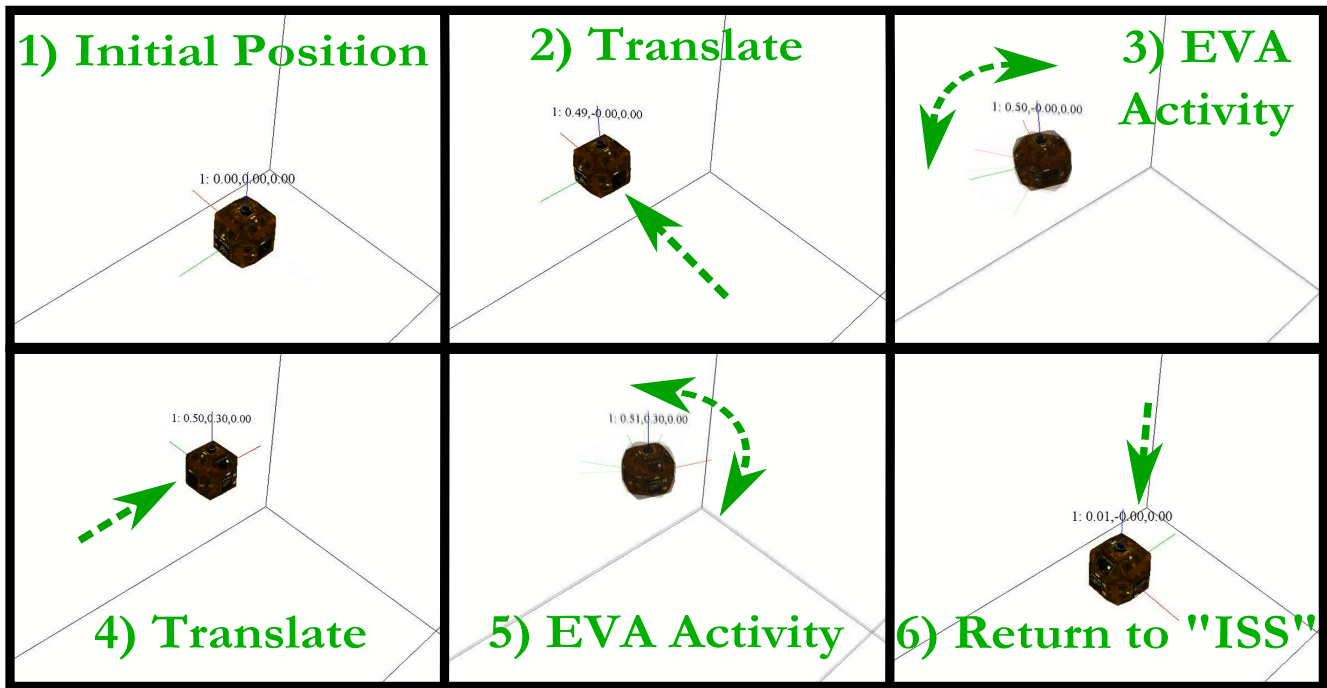


Fig. 22. A series of screenshots depicting a maneuver designed to imitate an astronaut conducting EVA maintenance activity at two different locations. This animation is quantitatively assessed in Figure 23.

rate of the thrusters. There are several mass flow rate numbers in the literature. Chen (2002) [15] empirically determined a mass flow rate of 0.378 grams/sec for a single thruster open, while a SPHERES technical document determined a value of 0.174 grams/sec (per thruster) with all 12 thrusters open. Because our trade study was first-order, we simply used the average of these two values for our final mass flow rate (0.276 grams/sec). The propellant mass saved for both the astronaut EVA maneuver and the SPHERES docked maneuver is listed in Table VI.

Additionally, if the system could be designed to carry less propellant due to the integrated CMGs, this would also lead to a reduction in tank mass. To estimate this mass savings, the “effective” tank mass used in the thrusters-only system was estimated as the original tank mass (440 grams) times the mass fraction of propellant used in the simulated maneuver (4.4 grams used/ 172 grams total for the astronaut EVA maneuver, 5.6 grams used/ 172 grams total for the docked maneuver). This resulted in a tank mass estimate of 11.3 grams needed for the thrusters-only actuated SPHERES to complete the astronaut EVA maneuver. The same calculations used on the combined CMG-thruster system resulted in a required tank mass of 6.9 grams. The propellant tank mass saved by adding CMGs is also listed in Table VI.

Each TORC-H86 CMG weighed 0.6 kg and the TORC controller board weighed 0.7 kg, for a total of 1.9 kg for the entire CMG scissor pair payload. As mentioned before, if this mass were simply compared to the propellant mass savings (a few grams), the trade-analysis would conclude that CMGs are not feasible. However, this comparison is not

appropriate: in the EVA maneuver described in Figures 22 and 23, the CMG gimbal angle reached a maximum absolute value of 0.072 radians, which is 4.6% of its maximum value of $\pi/2$ radians. Similarly, the average absolute gimbal rate was 0.0037 rad/sec, which is 0.19% of its maximum value of 2.0 rad/sec. These two values show that the CMG payload is underutilized by a significant factor, thus explaining why the mass of the CMG payload considerably outweighs the propellant mass savings.

For a fair comparison of the two options, the mass of the CMG payload was scaled down according to the gimbal angle usage to provide a better estimate of the true CMG payload required. That is, during the EVA maneuver the sine of the gimbal angle only reached 7.2% of its maximum value. This means that only 7.2% of the angular momentum envelope was utilized, so if the flywheel was 7.2% of its current mass, the CMG payload could have still performed adequately. The scaled-down mass is presented in Table VI.

Similarly, the CMG power usage had to be scaled down. Due to the complex nature of power consumption, we used the same scaling factor as described in the previous paragraph (momentum envelope utilization) as opposed to more sophisticated factors that would also account for average gimbal rate usage. This was done because this scaling factor was the most conservative measure. Scaling down CMG power resulted only 0.30W of the original 4W being ‘utilized’. This value was used as the average power consumption throughout the test session to generate the total energy used by the CMG payload (62.05 J). The total energy consumed by the CMG payload was used to calculate the battery mass needed using typical energy

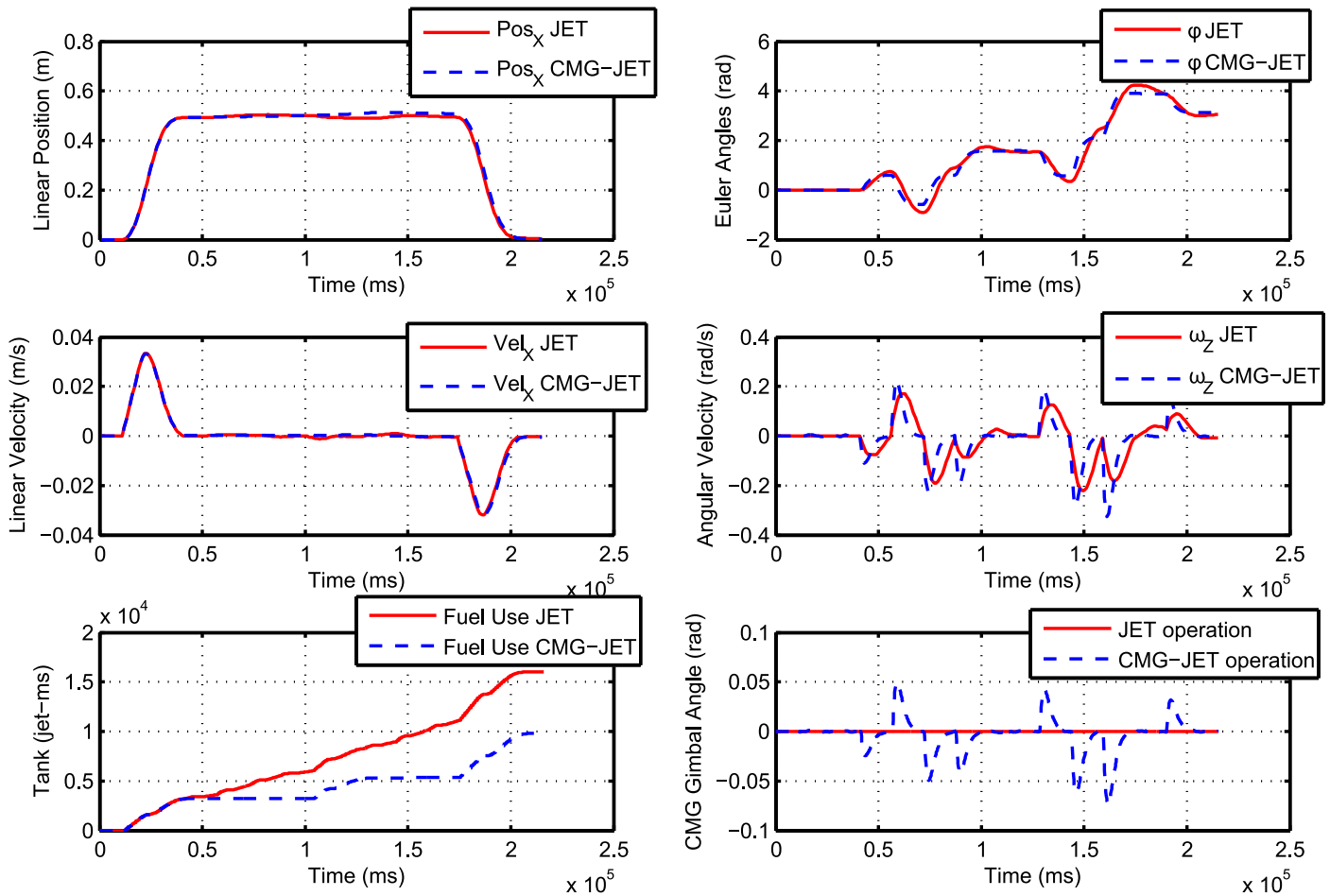


Fig. 23. From left to right, top to bottom: Plots of the linear position, angular position, linear velocity, angular velocity, propellant usage, and gimbal angle (or “CMG Usage”) for the SPHERES+CMG system (blue dashed line) and the SPHERES thrusters-only system (red solid line).

density values for Lithium-Ion batteries. Technical documents from Panasonic [16] gave a range of 0.36 to 0.95 MJ/kg, the mean of which was 0.66 MJ/kg. This means that an additional battery mass of 0.10 grams is required to support the CMG payload for this maneuver.

To reiterate, these calculations are only intended to provide an extremely rough estimate of the mass and power trade-off between the thrusters-only system and the combined CMG-thruster system. The scaling factors include many assumptions that are likely only true as first-order estimates, if that.

As we can see from Table VI, the mass trade analysis does not support the addition of CMGs. This result should be taken with the utmost caution, as it was highly dependent upon the scaling factors used. Future analysis should focus on developing a more accurate mass trade analysis.

V. FUTURE WORK

A. Air-Bearing Table Demonstration

Though the simulation emulates accurate communication protocols and CMG payload realism, significant work will be necessary to interface SPHERES with the CMG payload

hardware. Troubleshooting the SPHERES-CMG integration will be most easily conducted using a simple scissor-pair demonstration on the SSL’s air-bearing table, which only has 1 rotational degree of freedom. Two loaner TORC-H86 CMGs, which will arrive in the Spring 2014 semester, will need to be integrated with SPHERES and tested on an air carriage in the SSL. Apart from aligning the two CMGs’ gimbal axes to be parallel so that the horizontal components of angular momentum cancel each other out, there are no restrictions on how the loaner CMGs can be mounted to the air carriage. Software should ensure that the gimbal angles remain equal and opposite.

B. Halo Hardware Development

Structural analysis has not yet been performed on the mechanical design presented herein. Future work will be necessary to assess whether the four screw connection from interface plate / electronics enclosure to Halo is strong enough to withstand the torques capable of being produced by the CMGs in addition to the gravity forces during ground operation. Additionally, since flywheels require adequate containment when

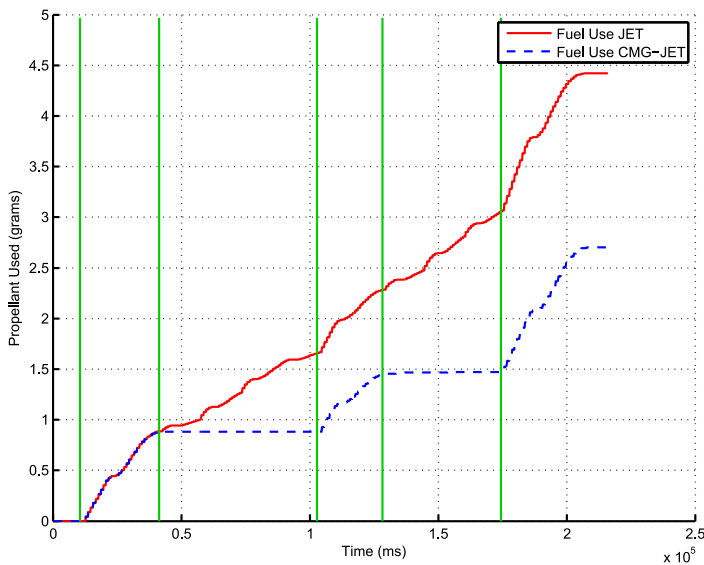


Fig. 24. The propellant used to conduct a simulated astronaut EVA maneuver using the SPHERES satellite with thrusters as the only actuator (red solid line) and with the combined thruster and CMG actuators (blue dashed line). This comparison clearly outlines the fuel saved by using CMGs to augment thruster actuation. The green vertical lines indicate the beginning and ending of maneuvers corresponding to figure 22.

TABLE VI. A SUMMARY OF THE MASS TRADE-OFFS INVOLVED IN ADDING A CMG PAYLOAD TO THE SPHERES SATELLITE TESTBED. THESE TRADE-OFFS ARE MANEUVER-DEPENDENT, AND ARE THUS PRESENTED FOR BOTH THE ‘EVA’ AND ‘DOCKED’ MANEUVERS.

CMG Payload Specs	EVA	Docked
Nominal Mass	1.9 kg	1.9 kg
‘Utilized’ Mass	136.3 g	1476.5 g
Nominal Power	4 W	4 W
‘Utilized’ Power	0.30 W	3.14 W
Add’l Batt Mass	0.10 g	1.68 g
CMG Added Mass	136.4 g	1478.2 g
Thruster Sys. Savings	EVA	Docked
Fuel Mass Saved	1.7 g (39%)	18.2 g (76%)
Tank Mass Saved	4.4 g	46.5 g
Thruster Mass Saved	6.1 g	64.8 g
Mission Duration	EVA	Docked
Thrusters-Only	2.3 hr	0.7 hr
Thrusters+CMGs	3.8 hr	3.0 hr
Duration Increase	1.5 hr (64%)	2.3 hr (325%)

operating in a microgravity environment including parabolic aircraft or the ISS, an investigation into the necessary strength of the CMG covers needs to be performed; this analysis will dictate their material and thickness.

Design of the connector PCB board (a placeholder for which is shown in Figure 9) needs to be completed. This connector board will need to perform conversion of the USB signal from Halo to RS-422 for the control board and to redirect the CMG connectors to the breakout locations.

C. Simulation Enhancements

The simulation will require several enhancements to increase its fidelity. First, the dynamics block in the simulation will need to be modified to include the angular momentum of the CMG array. That is, the rotational motion of the entire satellite will be more “sluggish” because the rotational motion will be inhibited by moving the angular momentum of the CMG array. This effect is non-existent in the air-bearing table system, because the satellite is limited to rotation around one axis, so the rotation vector and the CMG array’s angular momentum will always be parallel and this “sluggish” effect is dependent upon the cross-product.

Furthermore, any secondary effects of the CMGs on sensor readings (especially gyroscope readings on the IMU) will need to be studied and modelled in the simulation.

VI. CONCLUSION

This report has detailed the work completed by the SPHERES-CMG group in course 16.851 during the 2013 fall semester. This work is in direct support of the NASA/Draper effort to incorporate CMGs into future EVA jetpack designs with the purpose of decreasing fuel consumption and increasing EVA capabilities (as detailed in Section I). By developing a hardware demonstration that utilizes both thrusters and CMGs in a control system, this effort can contribute a significant step forward towards implementing such a design in EVA jetpacks. Many of the lessons learned in this project will prove useful to future work. This report first presented system requirements (in Section II) to communicate the scope and end deliverables of our project.

In Section III, a brief background was given on CMGs and the SPHERES satellite testbed. Various types of CMG arrays were surveyed and the scissor pair was selected for initial testing on the air-bearing table, while the box 90 and pyramid were selected for the final system capable of 3-DoF attitude control. The hardware team created a detailed CAD design that demonstrates how to mount an array of four CMGs on the Halo (shown in Figure 9). The final design not only avoids violating the “keep-out” zones of the thrusters and US/IR sensors on SPHERES, but also allows users to rotate the individual CMGs to enable either the box 90 or pyramid configuration. Momentum envelope calculations were carried out to ensure that the selected CMGs (in either configuration) could maintain appropriate control authority with the addition of the Halo hardware to SPHERES. The mass of each element of the design, down to the fasteners, was calculated to provide an initial mass estimate. This hardware design will act as a guide for future work attempting to integrate CMGs onto the Halo design.

Subsection III-G covers the work completed developing the electrical design. Commanding the CMG payload from the SPHERES controller requires sending data through the SPHERES expansion port, the VERTIGO computer, and the Halo USB network to the CMG control board. The pin layout of each interface was researched in order to determine the appropriate pin connections to use in establishing communication with the CMG payload. An adapter was identified that

would provide the proper interface between a Halo expansion port (USB) and the CMG control board (RS-422). The communication protocols of each interface were also researched to ensure that the integrated system would have compatible communication schemes. In addition to the communication system design, the power connection between the batteries on Halo and the CMG payload was detailed.

Following this, the work completed by the software team was presented in Section IV. This section presented a description of the current SPHERES simulation, as well as the approach taken by the software team to incorporate CMGs into the simulation. Special emphasis was placed on creating a simulation that would allow future users to easily test CMG+thruster control algorithms in a virtual environment before implementing them on the SPHERES hardware testbed. Two analogue astronaut EVA missions were simulated and the results are presented. The integration of CMGs into a jetpack was found to reduce the expended propellant and extend the achievable mission duration.

At the time of writing, the conceptual design and simulation have been completed, but the hardware demonstration was stalled due to a supplier delay. To address this, the report concluded with a description of anticipated future work that will allow future groups to achieve the project goals and requirements. Conducting a hardware demonstration of control algorithms utilizing thrusters and CMGs will be a large step forward in the endeavor of designing next-generation jetpacks that can utilize such control schemes. These designs will allow astronauts to explore objects in microgravity for prolonged periods of time with reduced jitter and improved stability.

APPENDIX A

JETPACK DEVELOPMENT: IN THE PAST AND TODAY

NASA's first jetpack development program took place in the late 1970s as part of the Skylab program [17]. Interestingly enough, the Manned Maneuvering Unit (MMU) of this development effort was initially designed to incorporate CMGs into a cold-gas actuated system in the M509 experiments [18], although the final design eliminated CMGs due to program constraints. Unfortunately, continued use of the MMU was canceled following the Challenger disaster in 1986. The jetpack system was later replaced by the system still used today, the Simplified Aid for EVA Rescue (SAFER), a compact unit to be used only in emergency egress situations [19], [20]. The SAFER unit is a powerful tool to protect the safety of astronauts but by the nature of its design it cannot support nominal EVA operations.

As stated in the report above, NASA has expressed an interest in the development of advanced human mobility systems, especially to support upcoming human exploration missions to near-Earth asteroids or other low gravity bodies [21]. Currently, Draper Laboratory and the Massachusetts Institute of Technology are designing a jetpack with integrated control moment gyroscopes (CMGs) for attitude control [2]. If sized and utilized properly, CMGs should significantly reduce fuel consumption at the expense of battery power and they should also ensure a more stable, stiffer working platform than

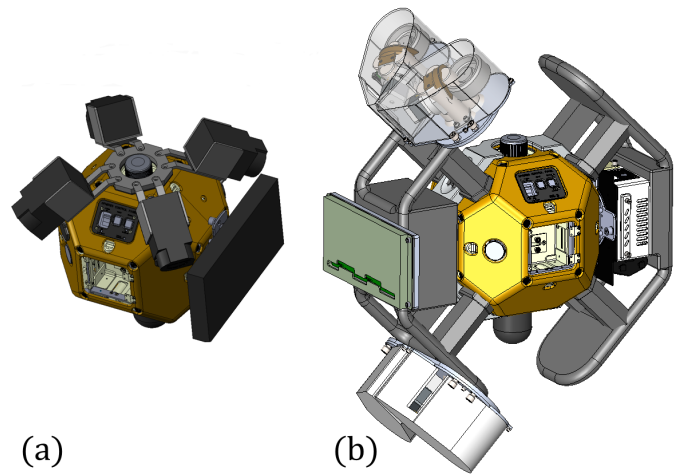


Fig. 25. Previous mechanical design iterations. (a) Pyramid array of Honeybee TORC-H86 CMGs on SPHERES without Halo. (b) Halo three port design shown in pyramid configuration.

a thruster-only system. In the Summer of 2013, Draper and MIT collaborated with NASA Johnston Space Center (JSC) to develop a virtual reality simulation of a theoretical CMG-jetpack system. After NASA astronauts tested this simulation in a variety of mission types, the simulation returned positive results: across all mission types, fuel consumption was reduced by 60-70% for CMG-jet actuation as compared with the jets-only actuation test cases [5].

It must be noted that the concept of integrating CMGs with cold gas jets into a mixed actuation system is not unique, and is in fact a common practice on spacecraft like the ISS or observational telescopes that require precise attitude control as well as translational control authority [22], [23], [24]. The recent development of small-scale (“mini”) CMGs has prompted a renewed interest in the idea of a CMG-integrated jetpack.

APPENDIX B

ALTERNATE MECHANICAL DESIGNS

The mechanical design presented in the main body of this paper is the last of several iterations. The most useful of these two iterations are the pyramidal (SPHERES only) design from [25] and the three port Halo design. These designs are shown in Figure 25.

Figure 25a shows a pyramid configuration using the Honeybee Robotics TORC-H86 CMGs, which are marginally smaller (600 g mass and 0.086 Nms momentum) than the LEO-H120 CMGs (700 g mass and 0.120 Nms). Here, the CMGs would fit over top of SPHERES, taking advantage of the 35.26° angles already present on the SPHERES satellite to create a pyramid CMG array. They would clamp against opposing sides of the SPHERES shell, contacting the shell with pads made out of rubber. This would provide a high friction surface to ensure that the CMGs would not detach in a microgravity environment. In a 1 g environment, the CMGs would sit atop SPHERES, with the black tank pointing down toward the floor

of the test area. A Honeybee Robotics provided control board would be attached to the expansion port.

Figure 25b shows a three port design for CMGs on Halo. This design is very similar to the one presented above. The differences are that the top and bottom CMG assemblies would be identical, and that the complexity of the connector PCB would be reduced. In this design, the connector PCB would only have to connect Halo to the host port of the CMG control board. It would not need to provide breakout connections for the other four ports as shown in the design presented in Section III-E.

APPENDIX C HALO KEEPOUT COMPLIANCE

The keepout zones are shown as cones in Figure 26. For the thrusters, these cones represent the volume over which the expansion of CO₂ occurs. For the ultrasonic sensors, these cones represent the ultrasonic “field of view”. The CMGs are shown in their box 90 configuration as the CMGs are most likely to interfere with the keepout zones in this configuration. Figure 26a and b show that the proposed design does not obstruct the thrusters. As can be seen in Figure 26c and d, the ultrasonic field of view is already largely obstructed by Halo. The addition of CMGs thus does not add significant interference with the keepout zones.

APPENDIX D CMG SAFETY ANALYSIS

This appendix details the safety analysis project conducted by Sam Schreiner as a part of the 16.842 Introduction to Systems Engineering course at MIT. This analysis follows the System-Theoretic Process Analysis (STPA) hazard analysis procedures [14].

System Introduction

CMGs will replace the thrusters as the primary actuator for attitude control (though the thrusters will still be used for translational/position control). The software on SPHERES is quite complex, so the integration of CMGs into the system warrants safety analysis to ensure that the system will still function properly after the integration.

The high-level functional goal of the CMG system is to control the attitude of the satellite by rotating a spinning flywheel around a gimbal axis. Though there are several possible CMG array architectures, the initial system will use a “scissor pair” array in which the two gimbal axis are parallel (or technically, anti-parallel) and the gimbal angles of the two CMGs are always equal, so the only component of the two flywheels’ angular momentum that does not cancel out is along a constant-direction vector. By mounting a CMG scissor pair such that the gimbal axis are in the horizontal plane, we can control the rotation of the SPHERES about the upward-pointing z-axis. This will allow us to conduct a hardware demonstration on the Space System Lab’s air-bearing table.

Potential Losses

The two major potential losses are incurring damage to the SPHERES satellites or to any humans nearby. Note: For this analysis, I am only considering operation in the SSL’s air-bearing table. This system is eventually destined for the ISS, which provides more hazards, such as damage the ISS and loss of prestige in public eye.

Potential Hazards (H)

H1: The CMGs cause SPHERES to spin too fast, saturating SPHERES IMU gyros (too much torque around upward axis). This dramatically reduces the accuracy of the attitude estimator and leaves the system open to the possibility of entering a hazardous spin that increases in speed.

H2: The two CMGs in the scissor pair become misaligned such that they generate a sufficient torque to tip over the SPHERES satellite (and the air-carriage it is hovering on) and cause damage (too much torque in horizontal plane).

H3: The CMG scissor pair gets into a state where it can no longer exert torques around the upward-pointing axis.

High-Level Constraints (C)

H1 ⇒ **C1a:** The spin rate around the z-axis must not exceed TBD.

H2 ⇒ **C2:** The CMGs must not exert a torque of more than TBD in the horizontal plane.

H3 ⇒ **C3:** The CMG gimbals must not become “locked up” (unable to generate any torque).

Functional Control Structure

The control loop for operating the integrated CMG-SPHERES system is shown in Figure 27, control loops not considered in this safety analysis are shaded.

The SPHERES controller is responsible for implementing most elements of the control. The process model in the SPHERES controller needs to contain a model of the current attitude of the SPHERES satellite as well as a model of the state of both CMGs. It must take in data from the Beacon Receivers and Inertial Measurement Unit (IMU) and combine this data to create an estimate of the attitude of the SPHERES satellite body (see below for more info). It also takes feedback from the CMG controller to determine the current state of the CMGs (the gimbal angle, gimbal rate, and flywheel speed of each CMG).

The SPHERES controller compares the satellite attitude estimate to the desired attitude of the satellite and, using this difference, determines the torque (vector) necessary to bring about the desired correction in state. This torque vector is translated into a gimbal rate command using the estimated state of the CMGs (determined from feedback from the CMG controller, as described above).

The CMG controller is grouped with its actuators (the 2 CMGs) to make the Inner CMG Control Loop. The contractor-built CMG controller is responsible for taking the commanded CMG state from the SPHERES controller and implementing it

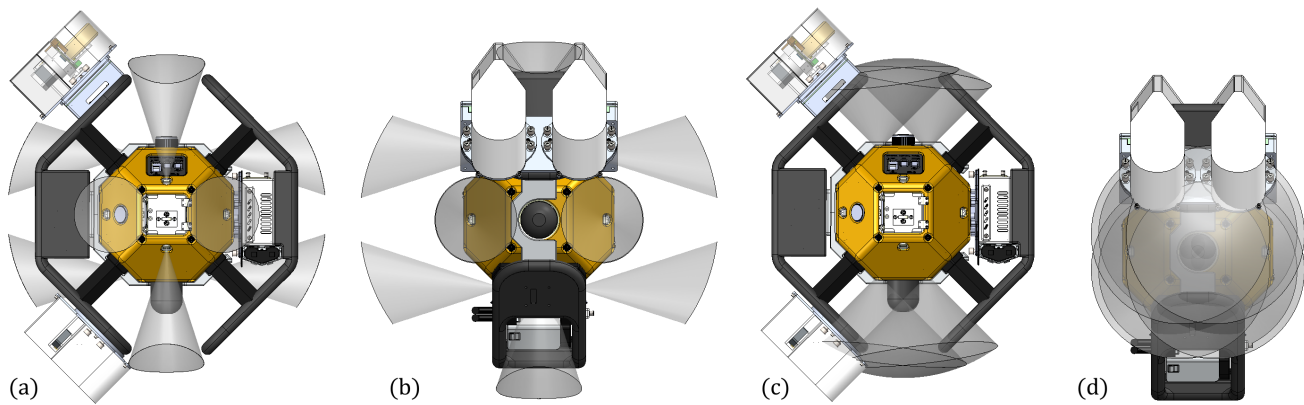


Fig. 26. Relevant Halo keepout zones shown with the CMG system in its box 90 configuration. (a) Right view of thruster keepout zones. (b) Bottom view of thruster keepout zones. (c) Right view of ultrasonic keepout zones. (d) Bottom view of ultrasonic keepout zones.

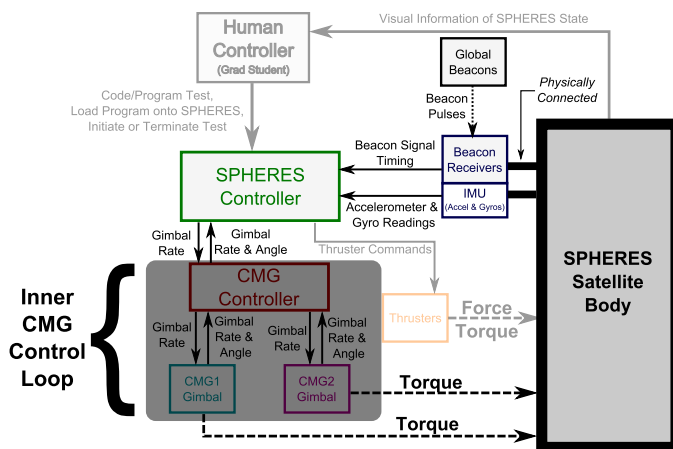


Fig. 27. An illustration of the SPHERES-CMG control loop used in the STPA safety analysis.

in the two CMGs. The CMG state has 2 degrees of freedom: rotation about the gimbal axis and rotation about the flywheel axis. For the control loop considered in this safety analysis, only control of rotation about the gimbal axis is considered (flywheel speed is usually just kept constant). For the purposes of this analysis, the CMG controller within this block can simply be considered to be a relay, but it commands and monitors the CMGs at a much higher frequency than the SPHERES controller.

For instance, if the SPHERES controller commands a gimbal rate of $2^\circ/\text{sec}$, the CMG controller relays this command to the CMG gimbal motor and also monitors the gimbal motor output at a much higher frequency than it receives gimbal rate commands from SPHERES.

Hazard 1 Analysis

In this subsection I build the Step 1 table (for STPA) for hazard **H1**: *The CMGs cause SPHERES to spin too fast, saturating SPHERES IMU gyros (too much torque around upward axis). This dramatically reduces the accuracy of the*

attitude estimator and leaves the system open to the possibility of entering a hazardous spin that increases in speed.

Shown in Table VII, the unsafe control actions **USC1** and **USC2** resulting from hazard **H1** generate safety requirement **R1a**: *The torque commanded to the CMGs must be antiparallel to the current spin rate (a negative sign in the proportional control law).* (This is standard control law design.)

Similarly, the unsafe control actions **USC1** and **USC2** resulting from hazard **H1** generate safety requirement **R1b**: *The lag in the control loop must be less than TBD milliseconds..*

H1-related Safety Constraints/Requirements:

Hazard 2 Analysis

In this subsection I build the Step 1 table (for STPA) for hazard **H2**: *The two CMGs in the scissor pair become misaligned such that they generate a sufficient torque to tip over the SPHERES satellite (and the air-carriage it is hovering on) and cause damage (too much torque in horizontal plane).*

Shown in Table VIII, the unsafe control action **USC2** resulting from hazard **H2** generates safety requirement **R2**: *The gimbal angles of both CMGs must be equal.*

Hazard 3 Analysis

In this subsection I build the Step 1 table (for STPA) for hazard **H3**: *The CMG scissor pair gets into a state where it can no longer exert torques around the upward-pointing axis (gimbal angle is close to $\pm 90^\circ$), the system loses control authority.*

Shown in Table IX, the unsafe control action **USC3** resulting from hazard **H3** generates safety requirement **R3**: *The gimbal angle (δ) must remain within the range of $\pm 90^\circ$ ($-90^\circ < \delta < +90^\circ$) at all times.*

Causes of Unsafe Control Actions

In this section I identify two possible causes of two of the unsafe control actions identified in the preceding section (**USC2** and **USC3**). **USC1** is not explicitly addressed because this unsafe control action is avoided by simply using a standard

TABLE VII. TABLE 1 FROM THE STPA SAFETY ANALYSIS - A LISTING OF THE UNSAFE CONTROL ACTIONS (USC) THAT CAN LEAD TO HAZARD 1 (H1): THE CMGS CAUSE SPHERES TO SPIN TOO FAST AND SATURATING THE RATE GYROS, LEADING TO THE LOSS OF ATTITUDE STATE ESTIMATE CAPABILITIES.

Control Command	Providing Control Command	Not Providing Control Command	Control Command Applied Too Soon/Late	Control Command Applied Too Long/Short
Increase/Decrease Gimbal Angle	USC1a: If satellite is spinning parallel to the commanded torque vector and the CMGs actuate, the satellite will spin faster.	USC1b: If the satellite is spinning anti-parallel to the commanded torque vector and the CMGs don't actuate, the satellite will spin faster.	USC1c: If the gimbal angle changes too soon/late, the phase angle between the control input and the spin behavior will grow, perhaps leading to unstable oscillations that result in too fast of a spin.	USC1d: If the gimbal is moved too long or too short, inadequate or excessive torques will be applied. This could cause the control law to be ineffective, allowing the spin rate to grow excessive.

TABLE VIII. TABLE 1 FROM THE STPA SAFETY ANALYSIS - A LISTING OF THE UNSAFE CONTROL ACTIONS (USC) THAT CAN LEAD TO HAZARD 2 (H2): THE CMG ARRAY CREATES A LARGE ENOUGH IN-PLANE TORQUE AND CAUSES SPHERES TO TIP OVER ON THE AIR-BEARING TABLE.

Control Command	Providing Control Command	Not Providing Control Command	Control Command Applied Too Soon/Late	Control Command Applied Too Long/Short
Increase/Decrease Gimbal Angle	USC2: If the two CMG gimbals actuate by TBD degrees/sec while misaligned by TBD degrees, they will generate a sufficient torque in the horizontal plane to tip over the SPHERES satellite on its stand	X	X	X

TABLE IX. TABLE 1 FROM THE STPA SAFETY ANALYSIS OF HAZARD 3 (H3): THE CMG SCISSOR PAIR GETS INTO A STATE WHERE IT CAN NO LONGER EXERT TORQUES AROUND THE UPWARD-POINTING AXIS (GIMBAL ANGLE IS CLOSE TO $\pm 90^\circ$), THE SYSTEM LOSES CONTROL AUTHORITY.

Control Command	Providing Control Command	Not Providing Control Command	Control Command Applied Too Soon/Late	Control Command Applied Too Long/Short
Increase/Decrease Gimbal Angle	USC3: If the gimbal angle is near $\pm 90^\circ$, a gimbal rate command could cause it to traverse 90° . This will cause the torque generated by gimbal rotation to flip sign, meaning the actual torque will be opposite in sign to the commanded torque. This can lead to unstable dynamic oscillations that grow in amplitude.	X	X	X

control law. This section presents possible “fixes” to the selected unsafe control actions.

I will first address **USC2**: *(If the two CMG gimbals actuate by TBD degrees/sec while misaligned by TBD degrees, they will generate a sufficient torque in the horizontal plane to tip over the SPHERES satellite on its stand.)*

The requirement generated to avoid this unsafe control action was **R2**: the gimbal angles of both CMGs must be equal. Given this requirement, one cause is that although the CMGs may start with the same gimbal angle and receive the same gimbal commands, as the test goes on the two gimbal angles may become unequal (in fact, it would be ridiculous to assume that they won't). This would probably be classified as actuator failure. So now we have to look at what the controller does if the gimbal angles are unequal. In this case, say gimbal angle 1 is $+10^\circ$ and gimbal angle 2 is $+12^\circ$. If the controller thought the gimbal angles were equal, it would issue a command based on a gimbal angle of $+11^\circ$, say, commanding a gimbal rate of $+2^\circ/\text{sec}$. My fix is for the controller to allocate a higher-than-nominal gimbal rate (say, $2.5^\circ/\text{sec}$) to gimbal 1 and a lower-than-nominal gimbal rate (say, $1.5^\circ/\text{sec}$) to gimbal 2. This is a crude estimate how a secondary controller needs to be implemented to maintain equal gimbal angles, but it may be enough, given that CMGs usually have very little friction in their motion (which is what would lead to unequal gimbal angles in the first place).

A second cause that could result in **USC3** could involve the timing of the implementation of the CMGs commands. The SPHERES controller interfaces with the actuator (the CMG control board + 2 CMGs) by sending 2 gimbal rates along the serial line. Thus, one command has to come after the other and, as such, one command will be received by the CMG controller before the other. Depending on the design of the CMG controller, it could implement the CMG commands as they are received, meaning that the first gimbal motor will actuate before the second. This could lead to a “wobble” in the torque vector generated by the CMGs which may induce unstable oscillations that grow in amplitude (worst-case). My fix is for the CMG controller to implement CMG gimbal commands at the same time, even though it receives them at different times. Although this perhaps may already be a standard in CMG controller design, this requirement will nevertheless be passed to the contractor responsible for the controller design.

Next I will address **USC3**: *If the gimbal angle is near $\pm 90^\circ$, a gimbal rate command could cause it to traverse 90° . This will cause the torque generated by gimbal rotation to flip sign, meaning the actual torque will be opposite in sign to the commanded torque. This can lead to unstable dynamic oscillations that grow in amplitude.*

The requirement generated to avoid this unsafe control action was **R3**: The gimbal angle (δ) must remain within the range of $\pm 90^\circ$ ($-90^\circ < \delta < +90^\circ$) at all times. Given this requirement, we see the potential for hazards nonetheless. Going around the control loop, if the CMG gimbals are at $+89.9^\circ$, and the SPHERES controller sends a gimbal rate command of $+10^\circ/\text{sec}$ (which is quite likely, because the control law determines gimbal rate proportional to the inverse of the

cosine of the gimbal angle, so as gimbal angle approaches 90° , the commanded gimbal rates will explode to infinity.). If this command is executed by the gimbal motor for ~ 200 milliseconds (typical period/frequency of the SPHERES controller), the gimbal angle will pass through 90° . Once the gimbal angle passes 90° , moving the gimbal in the positive direction will now create a torque of the opposite sign. This behavior is in taken into account in the controller code (it knows about the sign switch), so it will now command a negative gimbal rate to create a positive torque. One can imagine that this sort of behavior will result in the gimbal angle oscillating around 90° , while the CMG no longer generates any net torque. While this effect is taking place, whatever state the SPHERES satellite is in (that generated the need for a control command) will undoubtedly be increasing in magnitude, causing an increased demand for a control command. Thus, we can say with some certainty that the gimbal angle will not only oscillate around 90° , but that it will oscillate with increasing amplitude (bad!). My fix would involve putting a clause in the control code that states if the gimbal angle is within TBD degrees of $\pm 90^\circ$, the controller will no longer send gimbal rate commands (where TBD is dependent upon the product of the control period and maximum commandable gimbal rate). When this occurs, the control system will switch back to an old mode where the thrusters are responsible for providing control torques and the CMGs remain stationary.

Another cause is tied to the second hazard (the two CMGs become significantly misaligned). The CMG controller uses the average of both gimbal angles in the control law, so if one gimbal angle is 89.9° and the other is 80.1° , the CMG controller calculates the gimbal rate command off of the average gimbal angle (85°). This will lead to a gimbal rate command that will cause the gimbal at 89.9° to cross 90° and generate unanticipated torques. The fix for Unsafe Control Action 2 (above) will generally keep the CMG system from getting into this state, but if it fails we must design a new fix. My fix for this would be to have the control law always check to see if the calculated gimbal rate multiplied by the period of the control loop (and a certain safety factor) will result in the gimbal crossing 90° . If this is the case the controller should throw an error, cease gimbal operation, and transition to thruster-only mode (similar to the previous fix).

APPENDIX E ADDITIONAL SIMULATION RESULTS

The following plots (Figures 28-30) correspond to the docked SPHERES configuration simulation trials in which an active CMG-SPHERES system docked to an inactive SPHERE is commanded to translate 0.5m along a line orthogonal to the docking axis. Each plot contains six subplots: from left to right, top to bottom: linear position, angular position, linear velocity, angular velocity, propellant usage, and gimbal angle (or “CMG Usage”) for the SPHERES+CMG system (blue dashed line) and the SPHERES thrusters-only system (red solid line) as functions of time.

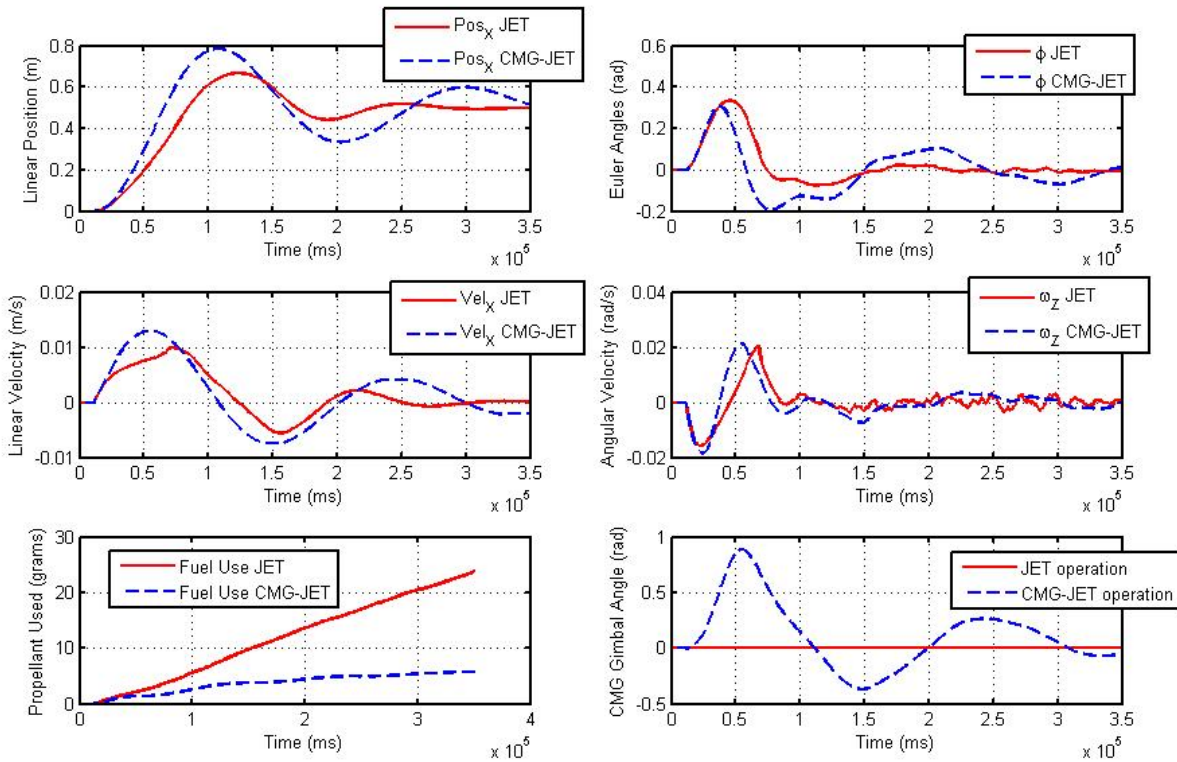


Fig. 28. Plot of simulation results for the case where jets-only operation performance is maximal and CMG+jets operation performance is tuned to match. This simulation's results are presented in the report to highlight the performance gains of using CMGs in conjunction with a cold gas system.

APPENDIX F SYSTEM REQUIREMENTS

This section provides a more detailed discussion of system requirements that guided the design of an integrated system using CMGs and thrusters on the SPHERES testbed. Aside from the top-level system requirements referenced in Table I, more concrete performance and operational requirements are included in this section.

Performance requirements for the CMG-SPHERES and CMG-SPHERES-Halo system are contained below in Table X. At the very least, in order for a CMG-integrated system to operate successfully in simulation and in experiment, attitude actuators, i.e. CMGs, must overcome external torques that correspond to maneuvers required of a CMG-jetpack system scaled to the CMG-SPHERES system. In the worst-case scenario, the system must remain functional even with a large externally-fixed inactive mass, represented in our case studies by an inactive SPHERE satellite. For more information about the scaling argument corresponding to this requirement as well as the derivation of torque and angular momentum requirements, please see Section III. In addition, minimal experimental success (though not simulation success) relies on CMGs not interfering with state estimators.

Basic system operation not only places requirements on the attitude control actuators, but also on the linear control actua-

tors, i.e. cold gas thrusters. For a CMG integrated SPHERES system to be minimally successful, thrusters must be able to overcome the inertia of the entire system mass. In other words, an unsuccessful system design would require such a long period of time to achieve translation that gas or batteries run out in SSL experiments, or that low gravity maneuvers can't be completed on experimental platforms like a parabolic aircraft or the ISS due to drift and time-constraints. The specific requirement of total system mass as indicated in P3 was derived from the following argument: At 40% duty cycle, the total force directed along one principle axis from SPHERES thrusters is 78.4 mN. Accounting (rather generously) for a friction force that negates 10% of this thrust, the total force transferred to the CMG-SPHERES system in any one direction for one thruster cycle is roughly 70.6 mN. If a 0.5 cm/s^2 linear acceleration is required from each thruster pulse, then, by solving for m in $F = ma$, $m = 14.1 \text{ kg}$. Note that for a duty cycle of 20% this mass limits linear acceleration to 0.25 cm/s^2 .

In addition to the requirements identified above, the attitude control of the CMG-SPHERES system should also meet requirements for precision (P2), time response (P5), and minimum drift (P6) to be maximally successful; likewise, the translation control of the CMG-SPHERES system should meet a similar requirement for precision (P4) and time response

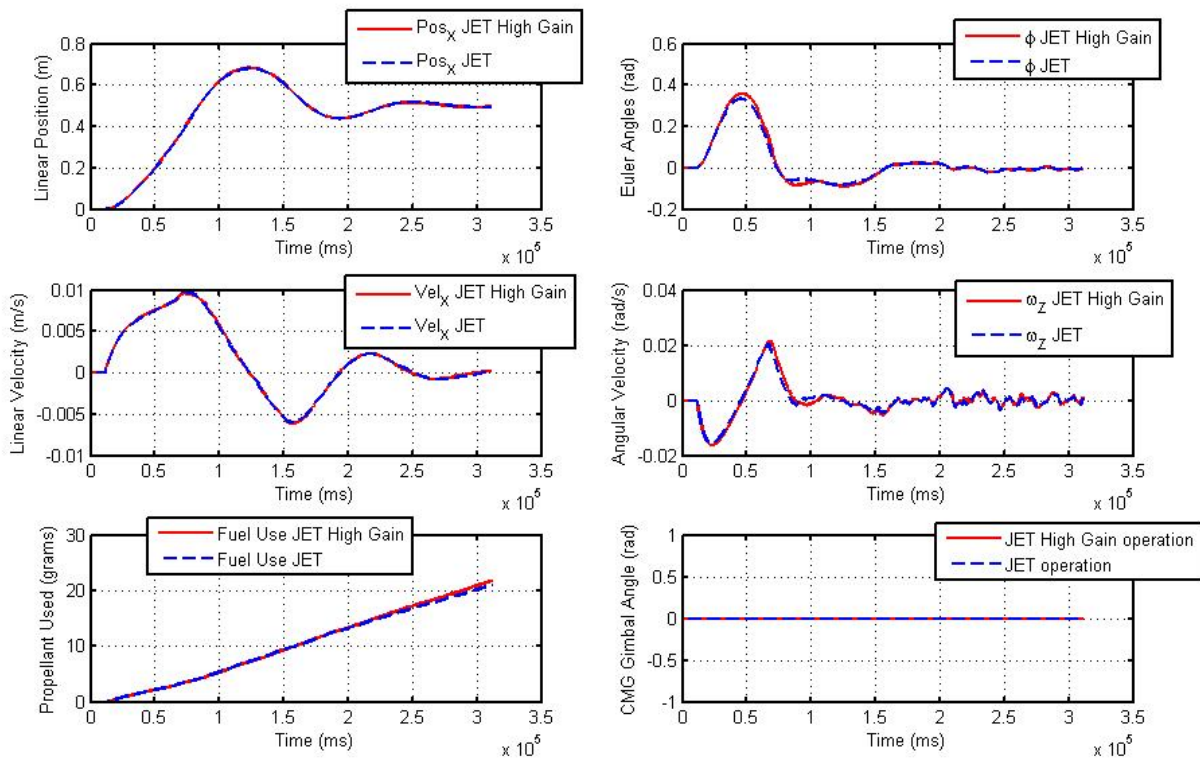


Fig. 29. Plot of simulation results for jet-only mode of operation: The dotted blue line corresponds to nominal position and attitude gains multiplied by factors of 3 and 75, respectively; the solid red line corresponds to nominal position and attitude gains multiplied by factors of 6 and 250, respectively. Note the nearly identical nature of both cases, indicating a maximal performance state has been reached using the lower gains.

(P5). It should be noted here that the precision requirement for the CMG-SPHERES-Halo system, $P2$ has been provided by the undergraduate 16.83 class as part of their project to design a specific CMG-SPHERES-Halo system to perform autonomous EVA inspection activities.

Finally, several key operational requirements and constraints have been included in Table XI, also located in this section. These requirements correspond to minimum lifetime, schedule, environmental, and top-level hardware demonstration requirements for the successful completion of the programmatic and experimental goals of the CMG-SPHERES program, a program that extends beyond the scope of the 16.851 team.

ACKNOWLEDGEMENTS

The authors would like to thank Dr. Jeff Hoffman and Dr. Babak Cohanim for their suggestions, critiques, and guidance during our weekly meetings. We thank Dr. Alvar Saenz-Otero and Dr. Dave Miller for sharing their expertise with the SPHERES testbed, as well as the SPHERES team for lending their time to support our software development efforts in particular. Thank you also to the Halo team for answering all of our questions and accommodating the needs of CMGs on Halo. A final thanks to Erik Mumm of Honeybee Robotics for his assistance in providing CMG designs and details.

REFERENCES

- [1] NASA Human Exploration Destination Systems Roadmap, 7.3: "Advanced" Human Mobility Systems, 7.3.3.4: Human Maneuvering Units.
- [2] M. Carpenter, K. Jackson, B. Cohanim, K. R. Duda, J. Rize, C. Dopart, J. Hoffman et al. *Next-Generation Maneuvering System with Control-Moment Gyroscopes for Extravehicular Activities Near Low-Gravity Objects*, AIAA 2013.
- [3] Saenz-Otero, Alvar. *Design Principles for the Development of Space Technology Maturation Laboratories Aboard the International Space Station*. Massachusetts Institute of Technology, 2005.
- [4] A complete list of SPHERES publications, including those related to low gravity experimentation aboard microgravity aircraft and the ISS can be found at: <http://ssl.mit.edu/spheres/papers.html>
- [5] Paper in preparation. M. Carpenter, K. Jackson, B. Cohanim, K. R. Duda, J. Rize, C. Dopart, J. Hoffman et al.
- [6] H. Kurokawa, *A Geometric Study of Single Gimbal Control Moment Gyros*, Report of Mechanical Engineering Laboratory, No. 175. Ministry of International Trade and Industry, Japan, 1998.
- [7] F. A. Leve, *Development of the spacecraft orientation buoyancy experimental kiosk*, MSc. University of Florida, 2008.
- [8] H. Yoon, *Spacecraft Attitude and Power Control Using Variable Speed Control Moment Gyros*, PhD Thesis, 2004, Georgia Tech
- [9] Saenz-Otero, Alvar. *SPHERES*. Massachusetts Institute of Technology, 2009. ssl.mit.edu/spheres/
- [10] Tweedle, Brent Edward, *Computer Vision-Based Localization and Mapping of an Unknown, Uncooperative, and Spinning Target for Spacecraft Proximity Operations*, PhD Thesis, 2013, MIT

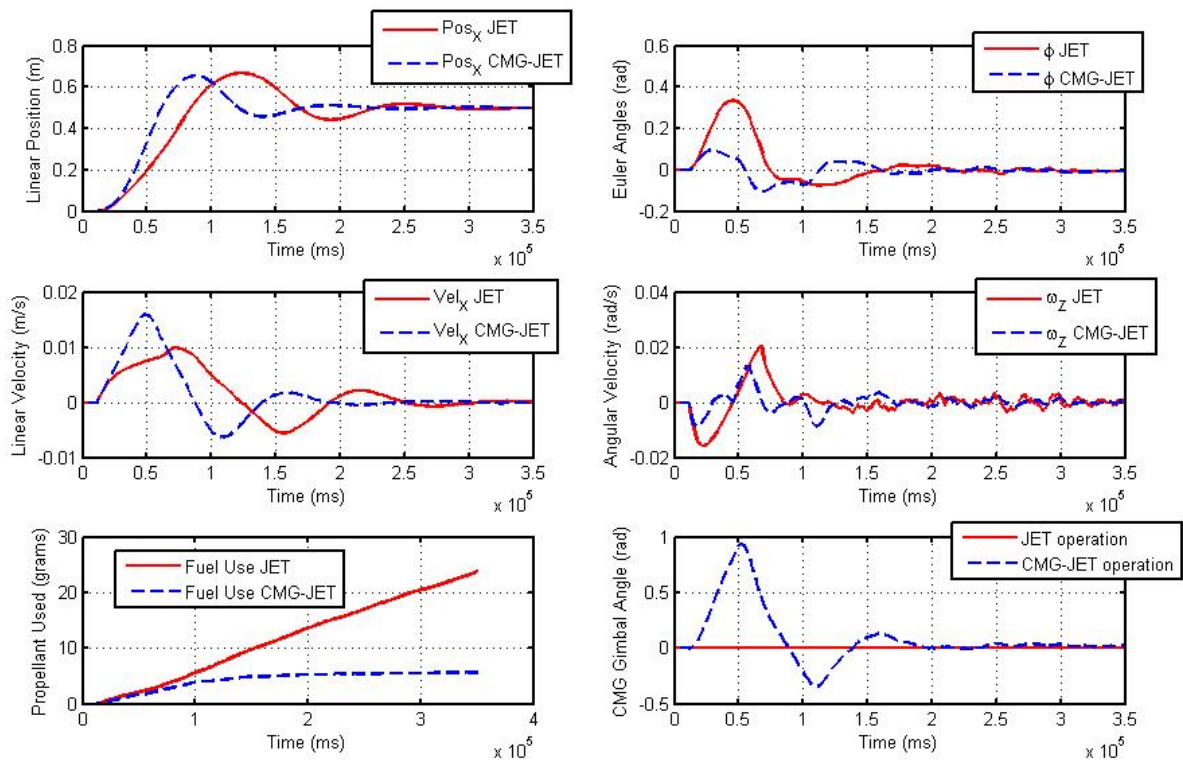


Fig. 30. Plot of simulation results for control algorithm implementation that yields the best performance for CMG+jet operation independently from the maximal performance of the jets-only mode of operation. Note the improved ability of the CMG+jets system to accommodate for induced torques.

- [11] J. Merk *SPHERES Expansion Port v2: Interface Control Document*, Aurora Flight Sciences, MIT Space Systems Laboratory, 2013.
- [12] *Vertigo Goggles Avionics Stack Interface Control Document*, MIT Space Systems Laboratory, 2013.
- [13] Ogata, Katsuhiko, *Modern Control Engineering, Fifth Edition*, Prentice Hall, 2009. Print.
- [14] Leveson, Nancy. *Engineering a safer world: Systems thinking applied to safety*. MIT Press, 2011.
- [15] Chen, Allen. *Propulsion System Characterization for the SPHERES Formation Flight and Docking Testbed*. Master's Thesis, May 2002.
- [16] Panasonic. *Overview of Lithium Ion Batteries*. http://www.panasonic.com/industrial/includes/pdf/Panasonic_LiIon_Overview.pdf. January, 2007.
- [17] Lenda, J. A., *Manned Maneuvering Unit: User's Guide*, NASA-CR-151864, May 1978.
- [18] Murtagh, T. B., Whitsett, C. E., Goodwin, M. A., and Greenlee, J. E., *Automatic Control of the Skylab Astronaut Maneuvering Research Vehicle*, Journal of Spacecraft and Rockets, Vol. 11, No. 5, May 1974, pp. 321-326.
- [19] Williams, T. and Baughman, D., *Self-Rescue Strategies for EVA Crewmembers Equipped with the SAFER Backpack*, NASA Goddard Space Flight Center, Flight Mechanics/Estimation Theory Symposium, No. N94-35633, May 1, 1994, pp. 357-371.
- [20] Vassigh, K., Weigel, D., and Mack, T., *USA Simplified Aid for EVA Rescue (SAFER) Operations Manual*, NASA Johnson Space Center, Systems Division, EVA Systems Group, JSC-26283 Rev. A, Aug. 20, 1998.
- [21] Chappell, Steven P., et al. *NEEMO 16: Evaluation of Techniques and Equipment for Human Exploration of Near-Earth Asteroids*. 44th Lunar and Planetary Science Conference. 2013.
- [22] Roithmayr, Carlos M. *International space station attitude control and energy storage experiment: effects of flywheel torque* National Aeronautics and Space Administration, Langley Research Center, 1999.
- [23] W. E. Haynes, *Control moment gyros for the space shuttle*, in Proc. IEEE Position Location Navigation Symp., New York, NY, 1984, pp. 1131-15.
- [24] Busseuil, Jacques, Michel Llibre, and Xavier Roser. *High Precision Mini-CMG's and their Spacecraft Applications*. AAS Guid. Control 98 (1998): 91-107.
- [25] S. Schreiner, T. Setterfield, T. Sheerin, M. Vanegas. *Hardware Demonstration of an Integrated CMG and Thruster Control System*. 16.851 Mid-term Report, October 11, 2013.

TABLE X. PERFORMANCE REQUIREMENTS

ID	Statement	Implication	Rationale	Verification
P1	System must provide adequate torque and angular momentum to control 2-SPHERES docked configuration	CMG sizing must be well-reasoned	Practical experimental constraint	Analysis, simulation and testing
P2	System must have attitude control precision of TBD degrees for jetpack demo, 0.5 degrees for INSPECT	CMG model selection, control implementation	Jetpack attitude control, INSPECT system nav requirements	Analysis, simulation and testing
P3	System mass should not far exceed 14 kg to ensure adequate linear acceleration (40% duty cycle 0.5 cm/s^2)	Minimize CMG array mass as much as possible	Practical experimental constraint	Analysis and testing
P4	Changes in thruster control will not negatively impact position control precision	Modifications to control algorithm must be conservative	Translational control must be effective	Analysis, simulation and testing
P5	System must respond to external disturbances to attitude and position in a timeframe TBD	Control timeline design constraints	System must simulate jetpack control requirements	Analysis, simulation and testing
P6	Relative drift between IMU and CMGs must be under a limit TBD	Periodic calibrations required	Experimental constraint	Analysis and testing
P7	CMG operation must not interfere with state estimation	Transient response time for CMG actuation must be known	Experimental constraint	Analysis and testing

TABLE XI. OPERATIONAL REQUIREMENTS AND CONSTRAINTS

Type	ID	Statement	Rationale	Verification
Lifetime	L1	System must remain with at least CMG battery power TBD and thruster fuel tank level TBD for at least t seconds	Experiment practicality	Analysis, simulation and testing
Schedule	S1	6-DoF controllable system design must be completed by the end of 2013, hardware demo by June 2013	Programmatic goal	Analysis
Environment	E1	System should be operable in MIT SSL on air-bearing table and on 3-DoF spike	Experimental goal	Analysis
Environment	E2	CMG-SPHERES-Halo system should be designed to accommodate modifications for zero-g flight or ISS operation	Programmatic, experimental goal	Analysis
Hardware Demo	H1	Multiple control algorithms, CMG configurations implementable for testing	Long-term programmatic, experimental goal	Simulation, design, analysis and testing